Reply to Reviewer 1

We thank Prof. Scherer for his very useful comments. We have addressed his comments below. We show how the text in the manuscript has changed, by indicating new text in boldface.

Comment: First of all, the entire study depends on the accuracy of downscaled precipitation. It would therefore be of utmost interest to better understand the uncertainties in the WRF output. As the authors correctly state, in-situ meteorological observations are scarce, and there is almost complete lack of data in the WKSK ranges, which makes it difficult to compare the WRF output with independent observations. This is especially true for high altitudes, i.e., the glacierized areas, where observational data are not available. Nevertheless, there are gridded data sets that could be used for comparison. Although they do not cover the entire study period (so far) and thus cannot substitute the ERA-Interim data used for downscaling, they could anyway be compared with the WRF results for shorter periods (as the authors have done with GLEAM data). The new ERA5 reanalysis and the High Asia Refined analysis (HAR) data set (Maussion et al., 2014) are suitable data sets in this respect. ERA5 data, especially the newest ERA5 land data set (https://cds.climate.copernicus.eu/cdsapp#!/dataset/reanalysis-era5-land?tab=overview), and the HAR data set do have very high spatial and temporal resolutions, such that they resolve mesoscale atmospheric processes, and thus orographically induced precipitation. HAR data are freely available at www.klima.tu-berlin.de/HAR. I would ask to authors to include a comparison of WRF output with these gridded data sets in the article. This could be put into a supplement with only a short paragraph in the main text.

Reply: We agree that such a comparison between different datasets will be a great addition to the manuscript, although we note that this does not necessarily increase the confidence in the results in WKSK, given the lack of ground truth for all these datasets.

We now added several paragraphs and two figures in the main text to deal with the comparison:

We also compare our WRF simulations with three similar data products with relatively high spatial resolutions, which have recently become available. We do note that all these datasets suffer from the lack of ground truth in WKSK, which means we cannot determine which dataset performs best in this region.

ERA5 is the follow-up of ERA-Interim (Copernicus Climate Change Service, 2017), with an improved spatial resolution of 0.25°, an improved temporal resolution, a more appropriate model input for e.g. sea surface temperatures, and more assimilated data. ERA5-Land is atmospherically forced by ERA5, and provides an even higher spatial resolution (0.1°) for land surface properties (Copernicus Climate Change Service (C3S), 2019). Finally, we include the HAR dataset with a resolution of 10 x 10 km, which uses WRF to downscale the NCEP FNR reanalysis dataset and re-initialises every day (Maussion et al., 2014). We compare temperatures between May-September, and annual precipitation, which give an indication of the parameters that are most relevant for glacier mass balance modelling. Because of the limited time overlap between the different datasets, we could only fully compare the period 2001-2010.

We binned all data to the same 0.5° x 0.5° grid to allow direct comparison. The mean values, trends, and interannual variability are compared in Figs. 3 and 4. It shows that ERA5 and ERA5-Land are nearly identical, and we only refer to ERA5 below. Our WRF model yields a warmer Karakoram than the other three datasets. Generally, the mean temperature differences are relatively minor, except for a warmer Tarim basin compared to HAR. We find very similar temperature trends as ERA5, although with smaller magnitudes. The magnitudes of the trends are also generally smaller than those in the station data (Fig. 2). The WRF interannual temperature variations correlate very well with ERA5, except two areas in the Tarim and the inner Tibetan Plateau. This is not surprising, given that our WRF model is forced by the similar ERA-Interim data. The whole western part of HMA, including WKSK, is especially well-correlated to ERA5. In that region, the correlation with HAR is weaker, but the correlation between HAR and our WRF data is very strong in East HMA. The differences with HAR might be explained by the different forcing, or by the difference in used physics modules, but this requires further study.

Differences between datasets are larger for precipitation, at least for the mean values and interannual variability. Our WRF simulations give results that are relatively wet in the Karakoram, and relatively dry in the Himalaya. However, the precipitation trends are very similar to ERA5 in both pattern and magnitude. An exception is the arid Tarim basin, which has an increasing trend in WRF, but a decreasing trend in ERA5. HAR shows a positive precipitation trend in most of HMA, with a very high trend in the Tarim basin. The correlation of the interannual variability is low in WKSK and parts of Tien Shan, which could be explained by the relatively high influence of the irrigated areas in the Tarim basin on the annual precipitation (de Kok et al., 2018, Fig. 3). Since our WRF model outcome is the only one of the four datasets that explicitly includes irrigation, this could explain the difference in annual variability.

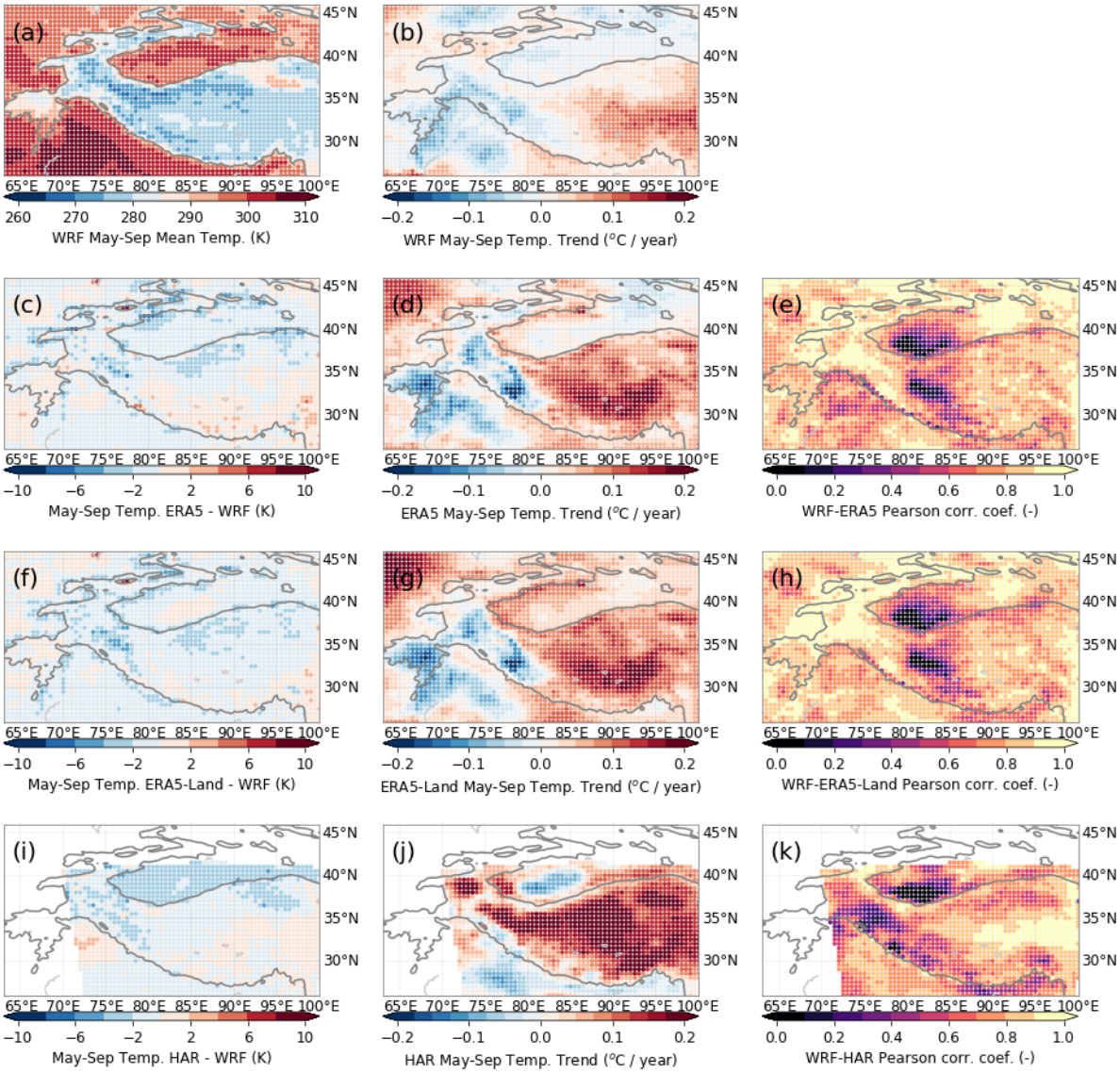

Figure 3: Comparison of WRF temperature output [a-b] with three other datasets (ERA5 [c-e], ERA5-Land [f-h], and HAR [i-k]). Columns show biases (c,f,i) with respect to the May-September mean temperature (a), May-September temperature trends (b,d,g,j), and Pearson correlation coefficients between the datasets and our WRF results (e,h,k). The 2000 m elevation contour is indicated by a solid line.

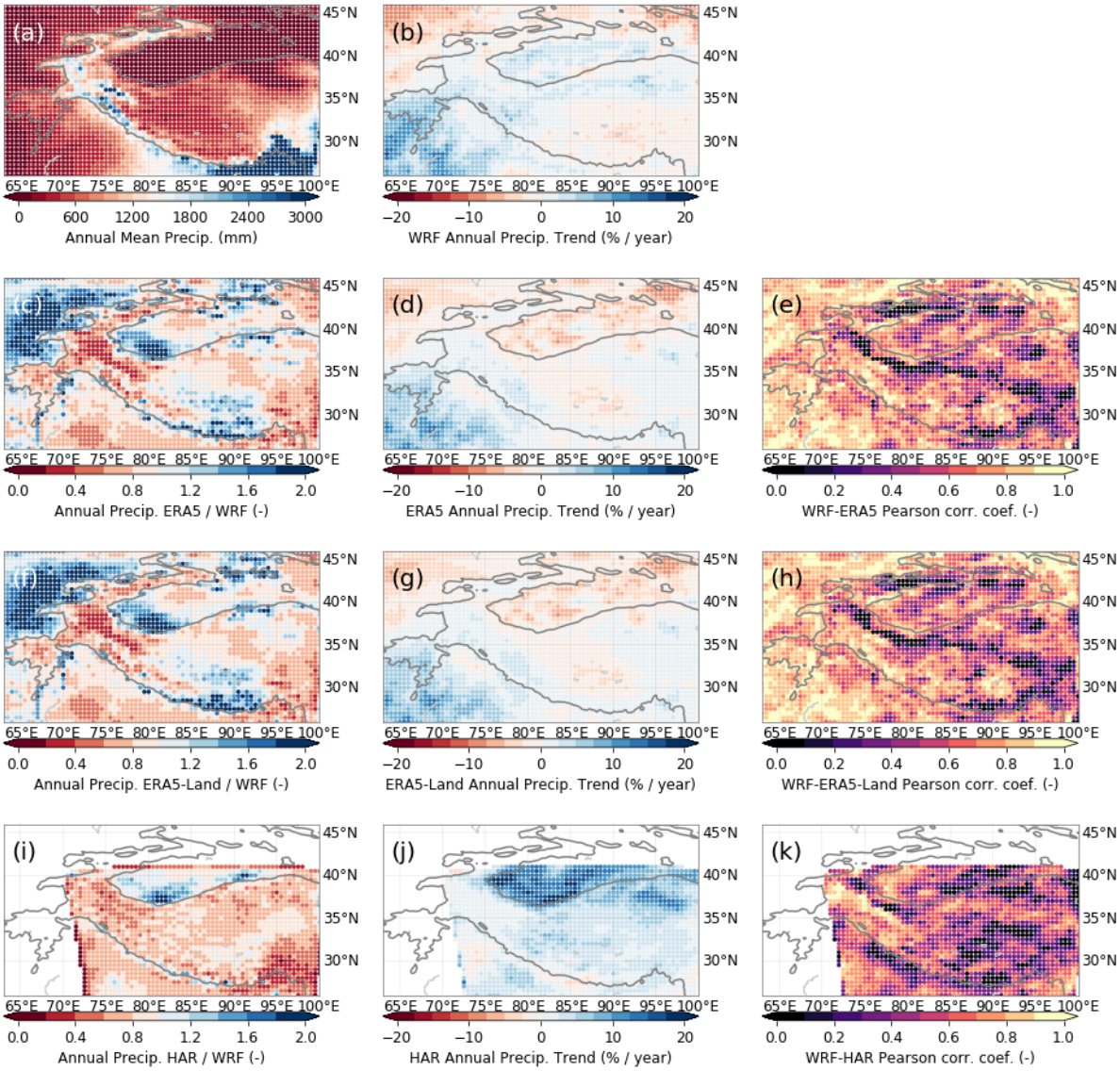

Figure 4: Comparison of WRF precipitation output [a-b] with three other datasets (ERA5 [c-e], ERA5-Land [f-h], and HAR [i-k]). Columns show precipitation multiplication factors (c,f,i) with respect to the annual mean precipitation (a), annual precipitation trends (b,d,g,j), and Pearson correlation coefficients between the datasets and our WRF results (e,h,k). The 2000 m elevation contour is indicated by a solid line.

In the discussion, we add: " **Our snowfall trends between 1980-2010 show some similarities, but also major differences with respect to a similar WRF study that did not include irrigation and used another re-analysis dataset (Norris et al.,**

2018). For instance, our temperature trends do not exhibit the strong summer cooling at low altitudes (e.g. the Tarim basin), and are more in line with station data (Waqas & Athar, 2018; Xu, Liu, Fu, & Chen, 2010) in that respect. However, contrasting precipitation trends in WKSK and southwestern HMA, similar to Fig. 5 *[now 6],* **are also present in ERA5 data and the Norris et al. study (see Farinotti et al. 2020). Although the interannual variability of temperature and precipitation is reasonably reproduced, and our precipitation trends are similar to those in other datasets, our model results are associated with uncertainties, which are partly irreconcilable due to a lack of *in situ* measurements in WKSK."**

Comment: The authors shall not only provide Pearson correlation coefficients but also further metrics like mean biases, r.m.s. deviations, regression slopes, etc., when comparing their WRF results with those from GHCN stations. I am not convinced that it is necessary to exclude so many GHCN stations by requesting at least 20 year of data coverage. This could be relaxed, or further comparisons may be added. I am also not convinced that it is sufficient to present results only for aggregated time periods, i.e., for annual mean air temperatures, May-September air temperatures, and July precipitation. Depending on the details of forcing the glacier model by WRF output, more detailed analyses of the WRF uncertainties are required, since snow- and ice melt can be rather variable from year to year, although years might have shown similar mean seasonal values for air temperature and precipitation.

In this respect, I would ask the authors to add more details on the WRF output and its application for forcing the glacier model simulations and the moisture tracking algorithm. In particular, I would like to know the output time step (one hour?).

Reply: It is true that the melt can be different per year. However, the glacier mass balance model does not include these subtleties. It requires a yearly input of temperature and snowfall and shifts the mass balance gradient accordingly to obtain an annual mass balance. In that sense, presentation of mean melt-season temperatures and annual mean precipitation is a reasonable representation of the data used in the glacier mass balance model. We already stated: "To modulate the mass balance gradient of the glacier over time, we applied annual precipitation changes derived from annual changes in WRF snowfall and temperature changes determined from annual changes in WRF melt season temperatures, i.e. when average daily temperature is above -5 °C. " We add a more detailed description of the glacier mass balance model as follows:

" To assess the response of the glaciers to the atmospheric forcing, we employ a glacier mass balance gradient model (Kraaijenbrink, Bierkens, Lutz, & Immerzeel, 2017). The model assumes a calibrated mass balance gradient along the glacier, and parameterises downslope mass flux in a lumped procedure that is based on vertical integration of Glen's flow law (Marshall et al., 2011). It also includes a parameterisation for the effects of supraglacial debris on surface mass balance (Kraaijenbrink et al., 2017), i.e. enhancing melt in the case of a shallow debris layer and limiting melt for thicker debris (Östrem, 1959). We modelled all individual glaciers in HMA larger than 0.4 km^2 (n=33,587) transiently for the period 1980-2010 (Kraaijenbrink et al., 2017). For ease of comparison with published observations, we select only those larger than 2 km^2 for the final analysis, which represent 95% of the glacier volume in HMA. Initial mass balance conditions in 1980 were set to be stable, while all other initial and reference conditions as described in the original study (Kraaijenbrink et al., 2017) were maintained. That is, using ERA-Interim data to locally calibrate the mass balance gradient of each glacier by constraining maximum ablation by a downscaled positive degree day climatology at the glacier terminus, and maximum accumulation by mean annual precipitation over the entire glacier area. The model simulates glacier mass change and evolution using a one-year time step, and hence requires representative annual input of temperature and precipitation. These are used to shift the mass balance curve according to sensitivity of the glacier's equilibrium line altitude to temperature changes, and adapt the maximum accumulation according to changes in precipitation (Kraaijenbrink et al., 2017)."

For the WRF output, we add: " **Results are output every 6 hours."**

Given, the annual input, we argue that it is then also reasonable to show the comparison with station data for the relevant aggregated temperature and precipitation data. Because of the mentioned difficulties with measuring snowfall accurately, we take the summer period. We now also took the period May-September, drop the 20 mm limit, and lower the number of available years to 15 to include more stations. Especially trends become very uncertain when few years are considered. The melt season used from the WRF output changes per location, but the summer months are likely to be most important. Hence, we compared these for the temperature data of the stations. Before describing the GHCN results, we add:

"Since the glacier model requires annual input, representation of the interannual variability is especially important. Any constant biases are of less importance, since we use relative interannual variations as input for the glacier model. However, biases in temperature will have an effect on the snow-rain partition."

Furthermore, we now add trends and biases into a new figure, which replaces Figures 2 and 3, and briefly discuss their results. We mention the median root-mean-square deviations in the text. We now write:

"We collected meteorological station data from **the Global Historical Climatology Network** (GHCN, Lawrimore et al., 2011, accessed June 2019), and selected those that have at least **15** years of full data between 1980-2010. **To be able to compare the WRF output with the station data, we apply a simple downscaling to the WRF temperatures in the grid that includes the station. We fit a linear temperature lapse rate to the temperatures and grid altitudes of a 2x2° box surrounding the station location. We then correct the WRF temperature by applying the lapse rate to the difference in altitude between the WRF grid and the station. Precipitation can also change significantly with location, but there is no clear relation between precipitation and altitude (Bonekamp et al., 2019; Collier and Immerzeel, 2015). For this simple comparison, we do not apply a downscaling of the WRF precipitation.**

Our WRF output produces May-September temperatures that are generally higher than the stations in the Tarim basin. However, biases are generally very low on the Tibetan Plateau, with values around 1°C. The median root-mean-square deviation between WRF and the stations is 1.8°C. The stations generally indicate a strong heating trend. Correlations between the annual variations in annual mean temperatures and mean temperatures between May-September are given in Fig. 2. They show generally very high correlations, with a lowest value of 0.5 (corresponding to $p = 0.005$). This implies that the interannual variability is very well reproduced in WRF. **This is despite the fact that many of these stations are situated in urban environments, with a potential heat island effect, a lack of evaporative cooling that is seen for irrigated agriculture, and a very difference surface energy balance than snow-covered areas. Hence, their locations might not be representative of the wider area, which might give rise to biases and trend differences when comparing the stations to the model outcome.**

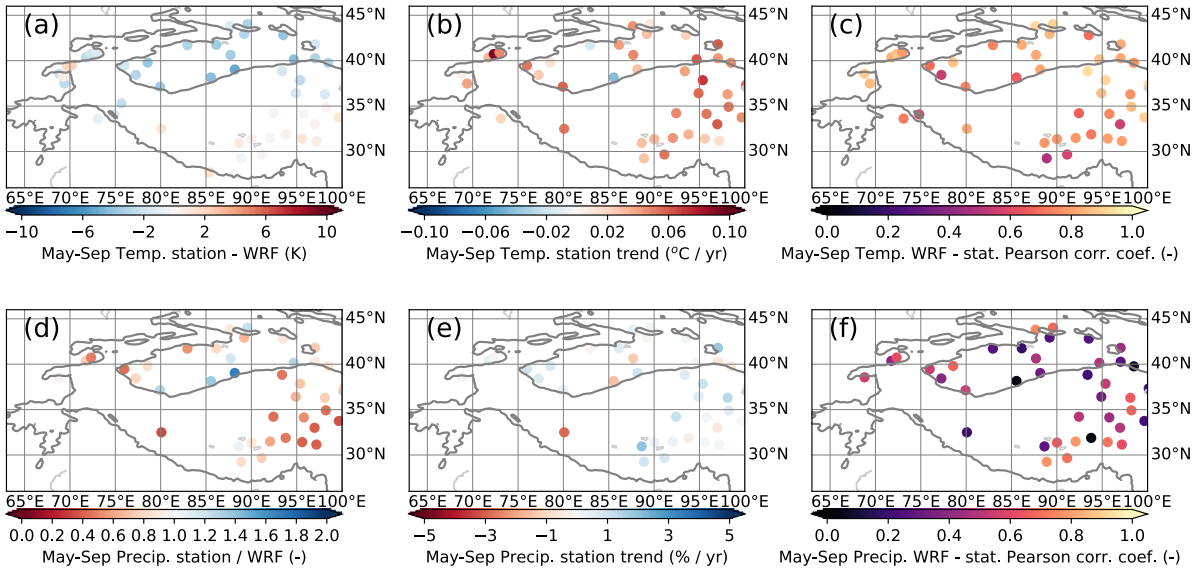

Figure 2: Comparisons between 1980-2010 time series of station data and nearest WRF grid for May-September temperatures (a-c) and May-September precipitation (d-f). Columns show temperature bias (a) and precipitation multiplication factor (d), trends (b,e) and Pearson correlation coefficients. The 2000 m-contour is indicated by a solid line

The stations in Fig. 2 closest to WKSK are almost exclusively in very arid regions, with a significant fraction of snowfall, **which is more difficult to reliably measure than rain (Archer, 1998),** making comparisons of precipitation very uncertain. Fig. 3 shows the **comparison** between time series of May-September precipitation, to limit the effect of snowfall. **Our WRF output is generally wetter than what is measured at the stations, except some locations in the Tarim basin. The median root-mean-square deviation between WRF and the stations is 11.4 mm per month. The stations show that most of the Tarim basin and Tibetan Plateau are seeing an increase in May-September precipitation.** The interannual variations are not represented by WRF as well as they are for temperature, but still show reasonable correlations for most stations, with values around 0.6. "

For the moisture tracking results, we selected the months that had the largest effect on the aggregated snowfall changes, as already stated in the text.

Reply to Reviewer 2

We thank the reviewer for the many useful comments. We have addressed the reviewer's comments below. We show how the text in the manuscript has changed, by indicating new text in boldface.

Comment: 1) In various figures (2,4,8,10,11,12), concise panel labels would be very helpful to allow the reader to immediately see what each panel shows, without having to read the caption.

Reply: We agree that this will help readability and have now added concise labels to all these figures, either in the figure or in the colour bar description.

Comment: 2) Similarly, in Figs. 6 and 7, a legend would be very helpful so the reader can immediately see what each line represents.

Reply: We agree that this will help readability and have now added legends to these figures.

Comment: 3) L54-55: By “the amount of irrigation needed to compensate evapotranspiration”, do you mean, after subtracting actual precipitation?

Reply: This is indeed the case, and we now indicate this as follows: "... compensate evapotranspiration, **after subtraction of the precipitation,** that..."

Comment: 4) L55: PCR-GLOBWB should be defined/spelled out.

Reply: We now add: "... that was calculated by the **PCRaster Global Water Balance model** (PCR-GLOBWB; ..."

Comment: 5) L71-73: How are these concentrations of the various greenhouse gases fed into the model? Is it through the radiation scheme?

Reply: This is indeed hard-coded in the radiation scheme, which we change for every year. We now state: "
210 Annual concentrations of CO_2, CH_4, and N_2O, **which are manually set in the RRTMG radiation module, ... "**

Comment: 6) L76: What is meant by "convergence between months"?

Reply: This was to check whether the monthly spin-up caused discontinuities in the time series. We rephrase
215 the sentence as follows: " We checked **whether temperatures and precipitation at the end of a month agreed with those at the end of the spin-up period for the subsequent month** and they agreed within a few percent for all selected points."

Comment: 7) L92: What is meant by "both deltas"?

220

Reply: We now rephrase the sentence as follows: "... the reference for **the changes in temperature and precipitation** was taken ..."

Comment: 8) L152-154: In this sentence, it sounds like the implicit assumption is that the measurements are
225 biased, but assuming these biases are constant in time, then we can use them to evaluate WRF's interannual variability. This should be made explicit.

Reply: It is not so much the problem that we assume a constant bias. Rather, it is the complete lack of data in the places where we are most interested in, meaning we can only compare it to measurements that are relatively
230 far away. We try to make this clearer by stating: " **Although not covering the glacierised areas of interest,** we compared our WRF output with data of the region **surrounding** WKSK, to ensure that the WRF output is a reasonable representation of the regional climate between 1980-2010."

Comment: 9) L156: GHCN has not been defined.

235

Reply: We now state: "... from **the Global Historical Climatology Network (GHCN) ..."**

Comment: 10) L159-160: Please explain the relevance of many of these stations being situated in urban environments.

Reply: We now state: " This implies that the interannual variability is very well reproduced in WRF. **This is despite the fact that many of these stations are situated in urban environments, with a potential heat island effect, a lack of evaporative cooling that is seen for irrigated agriculture, and a very difference surface energy balance than snow-covered areas. Hence, their locations might not be representative of the wider area, which might give rise to biases and trend differences when comparing the stations to the model outcome."**

Comment: 11) L166-167: Implicit in this sentence is that the stations measure snow less reliably than rain. Please make this explicit and provide a reference.

Reply: This is indeed the case. We now state: "... with a significant fraction of snowfall, **which is more difficult to reliably measure than rain (Archer, 1998),** making comparisons of precipitation very uncertain."

Comment: 12) L185: How do you know that the discrepancy is only in part due to the different spatial resolution? Have you quantified the effect of the spatial resolution?

Reply: We averaged over identical large areas to come to this conclusion. We now state this more explicitly: "... **as is evident from e.g. averaging over 1x1° areas**."

Comment: 13) Figure 6 is never referenced in a meaningful way. This figure shows nicely that there is no clear distinction between growing and shrinking glaciers in terms of temperature trends, but that there is a clear distinction in terms of snowfall trends. It would be nice to have some words to this effect in the text.

Reply: We agree and add: " **Fig. 6 shows that the trend and the interannual variability of temperature are very similar for nearby regions of both growing and shrinking glaciers.** The snowfall trends **in Fig. 5** have a very different pattern, with most of the Tibetan Plateau showing an increase and the western and southern mountain ranges, such as the Himalaya and the Hindu-Kush, showing a decrease in snowfall. **Furthermore, the mean level, the trend, and the interannual variability of snowfall is quite distinct for the two nearby regions of contrasting glacier mass balance trends.** "

Comment: 14) Figure 6 caption: how is representativeness of the bins determined?

Reply: The representativeness was not checked, but we simply picked two nearlby points with contrasting mass balances. We increased the representativeness by averaging over larger areas, and modify the caption as follows:

"...for two nearby 2x3° bins that have, on average, growing glaciers (38-40° N, 73-76° E, blue lines) and shrinking glaciers (35-37° N, 72-75° E, orange, dashed lines)."

Comment: 15) L230-232: It is quite confusing when you say "our simulations only go out to 2010, but we compare our results for 2000-2008". Why not compare results up to 2010? If 2008 is as far as the observations go, then the limitation is in the observations, not the simulations.

Reply: The phrasing was indeed confusing. The observations mostly go to periods later than 2010, but the 2000-2008 period was also given in Brun et al. (2017), although it is less accurate. We now rephrase as follows: " A more detailed quantitative comparison of the above results and the observed mass balances is hampered by the fact that our simulations only go out to 2010, **and hence we cannot compare with the most recent, and most accurate geodetic mass balance data. However,** we compare our results for the **intermediate** period 2000-2008, **as presented by Brun et al. (2017),** in Fig. 9."

Comment: 16) L232-233: As well as the model showing too little growth for the growing glaciers, it shows different glaciers growing to the ones in the observations (Fig. 9). Are the growing glaciers in the model and observations at least in the same areas?

Reply: They are indeed. We already mentioned: " In fact, all points where we model glacier growth in Fig. 8a also show growth or stable conditions in observations (Brun et al., 2017; Kääb et al., 2015), except one point in Kääb et al., (2015)." After the comparison in Fig. 9, we add: " **However, in both cases the growing glaciers are only present in the same region, mainly WKSK and the Tibetan Plateau."**

Comment: 17) L259: Presumably the low glacier temperature sensitivity in the WKSK is because, even with warming, temperatures in in the WKSK are still generally below freezing? This could be clarified. Or if there is a different reason?

Reply: Although such a narrative is sometimes employed, it is not really true that the glaciers in WKSK always experience negative temperatures. A glacier in balance loses as much mass by melt/sublimation as it has gained by snowfall, when averaged over a long period. Because the accumulation zone in WKSK is indeed very high, the glaciers need to extend down to warmer temperatures to be in balance. We now add: " The reduced temperature sensitivity is in line with previous work (Sakai & Fujita, 2017; Wang, Liu, Shangguan, Radic, & Zhang, 2019), **which argue that the generally large masses of the glaciers, and high equilibrium line altitudes, are important in explaining the lower temperature sensitivity in WKSK**. "

Comment: 18) I am slightly confused about Fig. 10b. Is temperature kept constant (similarly to snowfall being constant in Fig. 10a)? Please clarify in the caption.

Reply: This is indeed the case, and we now add, similar to 10a: " ... and a spatially uniform and constant snowfall increase of +0.5% yr^{-1} of the annual mean value**, with temperature kept constant** (b)."

Comment: 19) L279-280: The increases in the Tarim basin are just on the very edge of the basin. Can you confirm that the specific grid points that exhibit increases in moisture contributions have undergone an increase in irrigation?

Reply: These are indeed the irrigation areas. In our model, mainly the Yarkand area show largest increase in irrigation, which is very close to the edge of the basin. We now add: "The regions with the second largest increases are the areas in the Tarim basin **where irrigation has increased the most**, ..."

Comment: 20) L280: You say that the contribution is mainly in May to July, but only May is shown in Fig. 12.

Reply: We show May, because it is the month with the largest contribution to the increase in snowfall. We now clarify as follows: "... which contributes mainly in May-July, **with May showing the largest resulting increase in snowfall** (see Figs. 7 and 12)."

Comment: 21) L306-307: Do you mean the correlation is weaker because surface fluxes are lower in winter?

Reply: Mainly the snowfall is less in WKSK in winter. We now clarify as follows: " since this region contributes **relatively more** in winter (Fig. 12)**, when less snowfall reaches WKSK (Fig. 7)**."

Comment: 22) L335: After "Once the groundwater is depleted, the glaciers in WKSK will also receive less snowfall from this region", you should insert, "according to our results", or something similar.

Reply: We agree, and add the following: " Once the groundwater is depleted, **our results suggest that** the glaciers in WKSK will also receive less snowfall from this region, resulting in their retreat."

Comment: Technical corrections

1) L122: if→of
2) L126: "less than 1%" should be "more than 99%", unless I misunderstand?
3) L147: rare→sparse
4) L153: of→from
5) L185: extremes→maxima
6) Figure 5 caption: insert "annual" before snowfall. Same in other figures.
7) L214: think→thin
8) L215: northwestern→southwestern. Same on L295.
9) L229: Fig. 3a→Fig. 8a

Reply: We corrected all these technical issues as suggested by the reviewer, except point 3), which was correct (we talk about validation of our model, not validation from our model). We thank the reviewer for the very careful reading.

Reply to the editor

We thank the editor for also reading the paper very carefully and giving very useful feedback. We have addressed the editor's comments below. We show how the text in the manuscript has changed, by indicating new text in boldface.

Comment: (A) The model evaluation is not convincing – not due to the lack of observations (which is unavoidable), but because of the statistical methods used. One referee emphasizes the same problem. Please extend the model evaluation by metrics that quantify absolute differences (correlations only tell you about variabilities) and be more systematic (c.f., one referee is surprised that annual/May-Sep/and July precipitation are selected). The referee suggestions are very helpful in this regard. In the end, you should demonstrate to the reader that there is confidence in the model results and that they are not a mere model product but represent the real world.

Reply: Although comparing different datasets is certainly a useful exercise, convergence among datasets is not necessarily is a good measure of reliability or confidence in the model, if there is a lack of ground truth measurements. There is no good way of telling which dataset is closer to the truth in most of WKSK. However, we now add a much more detailed comparison with station data and other datasets, including 3 new figures. Please see the reply to Referee 1 for the implementation.

Comment: (B) The study is mostly descriptive, and the model output is hardly analysed in terms of processes that could explain the glacier and temperature/precipitation patterns. This approach also results from the fact that descriptions are often (too) short (as the paper was obviously compiled for a short-format journal in the beginning), which leaves some things unclear. Any efforts to expand in this respect would surely be appreciated by the future readers.

Reply: We partly disagree with this assessment. We explicitly used the moisture tracking algorithm to directly analyse the processes that could explain the differences in precipitation, which we show to be more important than differences in temperature. This direct approach means that there is less need for causes of the changes

in precipitation to be demonstrated indirectly or circumstantially, e.g. by showing figures of wind fields, evaporation trends, etc., as is commonly done.

We do agree that our descriptions are fairly concise. We did expand our paper by a fair amount before submitting to The Cryosphere (note that we have already included 12 figures in the manuscript), and we tried to be concise, yet complete. We now addressed all the specific issues that caused confusion by the referees, added more description of the glacier model, and we add more discussion on the role of the westerlies (see below).

Comment: 26: “but this alone cannot explain...” // any reference to support the statement?

Reply: We assumed the reader knows that the sensitivity of a system only influences the rate of response to a disturbance, and not the sign of the response. We try to clarify this by adding: "... but this alone cannot explain why some glaciers are actually growing, **since either a decrease of ablation or an increase in accumulation is needed**."

Comment: 63: Please justify why only the upper 35 levels are chosen for nudging

Reply: We add the following sentence: " **This ensures the large-scale upper-atmospheric circulation closely follows that of ERA-Interim, whereas near the surface, the model is more determined by the physics in WRF, e.g. evaporation in irrigated areas.** The **nudged levels and the** values of the nudging parameters have been found to perform well in similar studies ...**"**

Comment: 65: How do the nudging parameters compare to the standard values suggested by the developers?

Reply: We add the following sentence: " **The default values for all three parameters are 0.0003 s^{-1} in WRF."**

Comment: Section 2.1 and rest of paper: I am not sure that calling 20x20 km resolution “high” is still appropriate. It was fine some years ago (and I did so too), but in the meantime with growing computational power, km-scale runs over more than a decade are already available.

Reply: We agree. When we started work on this paper, full ERA5 data was not yet available, but things have indeed moved fast. We now rephrase the conflicting sentence in Section 2.1 as follows: **"...** to obtain a climate dataset between 1980-2010 for High Mountain Asia **with a resolution higher than that of ERA-Interim**." We could not find other instances where we claim the resolution to be high.

Comment: Section 2.2: Please clarify the ice dynamics part of the model. It is hard to understand from the current descriptions.

Reply: We now add: " **The model assumes a calibrated mass balance gradient along the glacier, and parameterises downslope mass flux in a lumped procedure that is based on vertical integration of Glen's flow law (Marshall et al., 2011)."**

Comment: 103: why are these three variables chosen for the clustering? I can't comprehend why it is a mix of surface variables and pressure-based variables.

Reply: This variable mix was chosen, because they are relevant for the glaciers on the surface, and for the moisture transport higher in the atmosphere. We now add: " **In this way, we delineate regions that have similar surface variables, relevant for the glaciers. Furthermore, these regions are also under the influence of similar winds, relevant for the moisture transport."**

Comment: 106: please say something like "(indicated later in Fig. 11)", otherwise it seems odd that Figure 11 comes after Figure 1.

Reply: We agree and add the "**later**".

Comment: 135-139: Is the conclusion correct? Even if one data set shows lower absolute values, it doesn't necessarily mean that a trend must also be lower. Please clarify.

Reply: This is indeed only the case when all values are scaled in the same way. We now add: **"..**. the absolute values of the trends will be lower in the WRF domain than outside **if there is a scaling factor in moisture flux between the**

two datasets. The trends in the Tarim basin will **then** be underestimated with respect to regions such as the Caspian Sea and the Junggar basin."

Comment: Section 3: Do your spatial patterns have any resemblance with those expected from strong westerlies influence as presented by Mölg et al. (2017, JGR Atmospheres, 122,3875–3891)? I am not raising this point because I am an author of that study, but because that study has a clear relevance with regard to the scientific content of your paper (westerlies should have an impact in the northwest of HMA).

Reply: This is indeed a very interesting point, and westerlies must indeed be important. This is also clear from Figs. 11 and 12, which show that most of the changes in precipitation in southwestern HMA, which mainly occurs in winter, correspond to source changes west of HMA. The pattern of precipitation trends indeed somewhat matches that expected from an increase in summer westerlies, as described by Mölg et al., but the situation is clearly more complex than simply a change in summer westerlies. We now discuss this issue in a new paragraph in the discussion:

The pattern of precipitation trends in Fig. 5b roughly matches the pattern that is expected from an increasing influence of summer westerlies, as shown by Mölg et al. (2017). These westerlies are also associated with strong heating and drying trends of the Indus Basin. An increase in irrigation also produces a very similar precipitation pattern, yet causes a cooling and wetting of the Indus Basin (de Kok et al., 2018). Our JAS trends of near-surface temperature and specific humidity (Fig. 13) indicate mostly cooling and wetting trends, which is more in line with the increase in irrigation than with the increase in summer westerlies. ERA5 data for JJA also indicates a similarly strong irrigation effect in the Indus basin (Farinotti et al., 2020). The moisture tracking results (Figs. 11 and 12) indicate that much of the additional snowfall occurs in spring and summer, and originates from the East, with a large role for the irrigated areas. However, the May westerlies clearly have an important role in transporting the increase in evaporation from the Caspian Sea (Chen et al., 2017) to WKSK. Besides the Caspian Sea, the westerlies are mainly associated with a decrease in snowfall when the whole year is considered (Fig. 11a). The pattern of precipitation trends in Fig. 5b is not only the result of changes in summer. The decrease in precipitation in southwestern HMA is also clearly associated with westerly winds in winter, but not those in summer (see Figs. 7d and 11c).

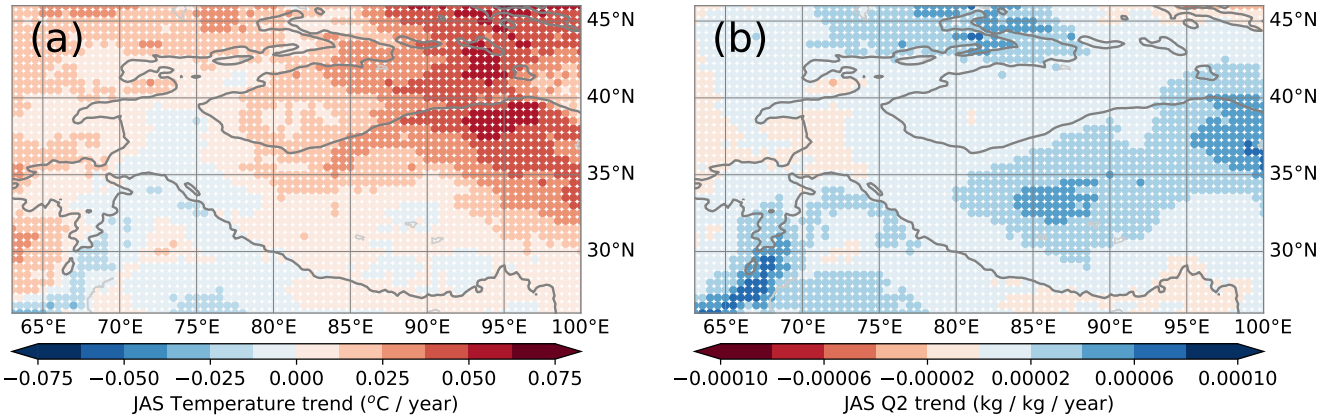

Figure 13: Trends between 1980-2010 of near-surface temperature (a) and specific humidity (b) between July-September, averaged over 0.5x0.5° bins for clarity. The 2000 m elevation contour is indicated by a solid line.

480

Comment: 175: Suggest “variable” instead of “parameter”

Reply: We changed the text as suggested.

485 **Comment:** 255: Many glaciers switch from red to blue; is this really a “minor effect”?

Reply: The figure shows that the effect of precipitation is smaller than the effect of temperature. We try to clarify the sentence as follows: "... temperature, **while the decrease in precipitation gives a much smaller mass balance response in this region**.

490

Comment: 291: The description implies that -0.4 or -0.6 should also be white, which is not the case. Please correct the caption

Reply: We add "absolute" before "magnitude".

495

Snowfall increase counters glacier demise in Kunlun Shan and Karakoram

Remco J. de Kok[1], Philip D.A. Kraaijenbrink[1], Obbe A. Tuinenburg[2], Pleun N.J. Bonekamp[1], Walter W. Immerzeel[1]

[1]Department of Physical Geography, Utrecht University, Utrecht, PO Box 80115, 3508 TC, The Netherlands
[2]Copernicus Institute of Sustainable Development, Utrecht University, Utrecht, PO Box 80115, 3508 TC, The Netherlands

Correspondence to: Remco J. de Kok (r.j.dekok@uu.nl)

Abstract. Glaciers in High Mountain Asia provide an important water resource for communities downstream and they are markedly impacted by global warming, yet there is a lack in understanding of the observed glacier mass balances and their spatial variability. In particular, the glaciers in the western Kunlun Shan and Karakoram ranges (WKSK) show neutral to positive mass balances despite global warming. Using models of the regional climate and glacier mass balance, we reproduce the observed patterns of glacier mass balance in High Mountain Asia of the last decades. We show that low temperature sensitivities of glaciers and an increase in snowfall, for a large part caused by increases in evapotranspiration from irrigated agriculture, result in positive mass balances in WKSK. The pattern of mass balances in High Mountain Asia can thus be understood from the combination of changes in climatic forcing and glacier properties, with an important role for irrigated agriculture.

1. Introduction

Glaciers in High Mountain Asia (HMA, see Fig. 1) show a very diverse response to the changing climate. Most glaciers are losing mass, as expected, but surprisingly, glaciers are stable or growing in a region northwest of the Tibetan plateau, a phenomenon dubbed the Karakoram anomaly (Hewitt, 2005). Recent studies have mapped glacier mass losses and velocity changes in detail and have shown that the regions of largest glacier growth and acceleration are the Kunlun Shan and parts of the Pamir, with the glaciers in Karakoram being close to a steady state (Brun et al., 2017; Dehecq et al., 2019; Gardelle et al., 2012, 2013; Kääb et al., 2015; Lin et al., 2017). Part of the mass balance variability seems correlated to differences in the temperature sensitivity, i.e. the change of mass balance for a certain change in temperature, of the glaciers (Sakai and Fujita, 2017), but this alone cannot explain why some glaciers are actually growing, **since either a decrease of ablation or an increase in accumulation is needed**.

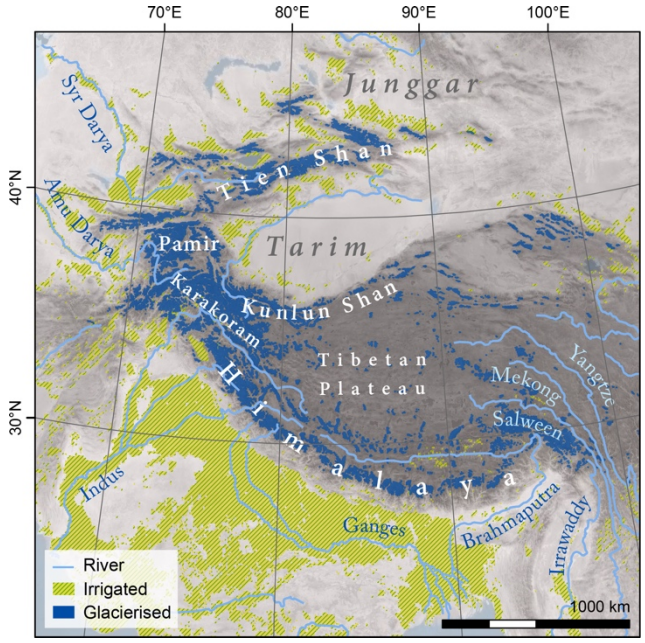

525 **Figure 1: Map of study area. Irrigated areas (from GMIA (Siebert et al., 2010)) and glacierised areas (from RGI 6.0 (Pfeffer et al., 2014)) are indicated.**

Suggested causes of the Karakoram anomaly include an increase in winter snowfall (Cannon et al., 2015; Kapnick et al., 2014; Norris et al., 2015, 2018), summertime cooling (Bocchiola and Diolaiuti, 2013; Forsythe et al., 2017; Fowler and Archer, 2006; 530 Khattak et al., 2011; Ul Hasson et al., 2017), and an increase in summertime precipitation and clouds due to irrigation in the agricultural regions adjacent to the Kunlun Shan and Pamir (de Kok et al., 2018). So far, these hypotheses have only tried to explain the Karakoram anomaly in qualitative terms, identifying possible climatic conditions that could lead to glacier growth. None of these have yet been able to directly reproduce the observed pattern of glacier mass balances in HMA directly by showing the response of the glaciers to the historic climatic forcing. Here, we simulate glacier mass balances using modelled 535 time series of temperature and snowfall from a regional climate model to reproduce the pattern of observed mass balances in HMA, and to more deeply understand the underlying causes.

2. Methods

2.1 Regional climate model

540 Irrigation can influence the regional and global climate (Cook et al., 2015; Lee et al., 2011; Lobell et al., 2008; Puma and Cook, 2010; Sacks et al., 2009). Since the regions surrounding HMA host the largest irrigated areas in the world, e.g. the Indo-Gangetic Plain (see Fig. 1), irrigation potentially influences the regional climate in HMA (Cai et al., 2019; de Kok et al., 2018).

However, available re-analysis datasets do not fully include irrigation, and generally have a relatively coarse spatial resolution. Hence, we downscaled ERA-Interim (Dee et al., 2011) re-analysis data using the Weather Research and Forecasting model (WRF, Skamarock & Klemp, 2008) to obtain a climate dataset between 1980-2010 for High Mountain Asia **with a resolution higher than that of ERA-Interim**. We artificially applied irrigation to the surface by adding a precipitation term each time step, with a rate that is determined per month. The amount of irrigation applied per grid cell was based on the monthly water demand, which indicates the amount of irrigation needed to compensate evapotranspiration, **after subtraction of the precipitation,** that was calculated by the **PCRaster Global Water Balance model** (PCR-GLOBWB; van Beek & Bierkens, 2008; van Beek, Wada, & Bierkens, 2011; Van der Esch et al., 2017; Y. Wada, Wisser, & Bierkens, 2014; Yoshihide Wada et al., 2011). In this way, the irrigation amount is not easily overestimated, as could be the case when e.g. soil moisture would be kept constant. In reality, insufficient water might be available to meet the predicted demand, whereas inefficient irrigation will result in a larger water gift than predicted.

We used WRF, version 3.8.1, to downscale ERA-Interim data to a resolution of 20x20 km, with 50 vertical levels. Settings are nearly identical to our previous work (de Kok et al., 2018), and are shown in Table 1. Additionally, we now use grid nudging of the upper 35 vertical levels for horizontal wind, temperature, and humidity, as opposed to only forcing the model at the boundary in our previous study. **This ensures the large-scale upper-atmospheric circulation closely follows that of ERA-Interim, whereas near the surface, the model is more determined by the physics in WRF, e.g. evaporation in irrigated areas.** The **nudged levels and the** values of the nudging parameters have been found to perform well in similar studies (Collier and Immerzeel, 2015; Otte et al., 2012), and are: 0.0001, 0.0001, and 0.00005 s^{-1} for horizontal winds, temperature and water vapour, respectively. **The default values for all three parameters are 0.0003 s^{-1} in WRF.**

Table 1: Physics modules and assumptions used in WRF.

Module	Setting
Radiation	RRTMG scheme (Iacono et al., 2008)
Microphysics	Morrison scheme (Morrison et al., 2009)
Cumulus	Kain-Fritsch (new Eta) scheme (Kain, 2004)
Planetary boundary layer	YSU scheme (Hong et al., 2006)
Atmospheric surface layer	MM5 Monin-Obukhov scheme (Beljaars, 1995; Dyer and Hicks, 1970; Paulson, 1970; Webb, 1970; Zhang and Anthes, 1982)
Land surface	Noah-MP (Niu et al., 2011)
Top boundary condition	Rayleigh damping
Diffusion	Calculated in physical space

Annual concentrations of CO_2, CH_4, and N_2O, **which are manually set in the RRTMG radiation module,** are derived from NOAA (Dlugokencky et al., 2018) and AGAGE (Prinn et al., 2000) data, as aggregated by the European Environment Agency (www.eea.europa.eu, accessed March 2018), and are kept constant throughout each year. We used a 10-day spin-up for each month and run each month separately to be able to include a different irrigation amount each month. Monthly initialisation of the snow cover, surface and soil temperature, and surface moisture was taken from GLDAS 2.0 (Rodell et al., 2004) monthly mean values. We checked **whether temperatures and precipitation at the end of a month agreed with those at the end of the spin-up period for the subsequent month** and they agreed within a few percent for all selected points. **Results are output every 6 hours.**

2.2 Glacier model

To assess the response of the glaciers to the atmospheric forcing, we employ a glacier mass balance gradient model (Kraaijenbrink et al., 2017). The model assumes a calibrated mass balance gradient along the glacier, and parameterises downslope mass flux in a lumped procedure that is based on vertical integration of Glen's flow law (Marshall et al., 2011). It also includes a parameterisation for the effects of supraglacial debris on surface mass balance (Kraaijenbrink et al., 2017), i.e. enhancing melt in the case of a shallow debris layer and limiting melt for thicker debris (östrem, 1959). We modelled all individual glaciers in HMA larger than 0.4 km^2 (n=33,587) transiently for the period 1980-2010 (Kraaijenbrink et al., 2017). For ease of comparison with published observations, we select only those larger than 2 km^2 for the final analysis, which represent 95% of the glacier volume in HMA. Initial mass balance conditions in 1980 were set to be stable, while all other initial and reference conditions as described in the original study (Kraaijenbrink et al., 2017) were maintained. That is, using ERA-Interim data to locally calibrate the mass balance gradient of each glacier by constraining maximum ablation by a downscaled positive degree day climatology at the glacier terminus, and maximum accumulation by mean annual precipitation over the entire glacier area. The model simulates glacier mass change and evolution using a one-year time step, and hence requires representative annual input of temperature and precipitation. These are used to shift the mass balance curve according to sensitivity of the glacier's equilibrium line altitude to temperature changes, and adapt the maximum accumulation according to changes in precipitation (Kraaijenbrink et al., 2017).

To modulate the curve transiently, we applied annual precipitation changes derived from annual changes in WRF snowfall and temperature changes determined from annual changes in WRF melt season temperatures, i.e. when average daily temperature is above -5 °C. A threshold value of 0 °C did not significantly change the glacier mass balance results for most of HMA, but meant that temperature changes for the coldest points could not be determined, since they are always below 0 °C.

We did not take into account whether the WRF grid point was glacierised or not. To reduce potential biases imposed by spurious reference conditions, the reference for **the changes in temperature and precipitation** was taken to be the average of the first six modelling years, i.e. 1980-1985. We performed three separate glacier model runs to evaluate the attribution of snow and temperature to the glacier mass changes in our model, forced by: (1) precipitation and temperature, (2) only temperature, and (3) only snow. To illustrate the temperature and precipitation sensitivity of the glaciers, we also performed calculations using a fixed temperature or snowfall trend for all of HMA, with the other variable kept constant.

2.3 Moisture tracking

Our moisture tracking model (Tuinenburg et al., 2012) follows the moisture associated with precipitation backwards in time to determine where the moisture first enters the atmosphere. It therefore establishes a direct causal link between evapotranspiration and precipitation downwind. For the moisture tracking, we clustered locations that have similar climates in terms of seasonality, since these will likely also have similar moisture sources. For the clustering, we used the monthly mean values of precipitation, horizontal wind fields at 400 hPa, and 2m-temperatures, with means subtracted and divided by the standard deviations, to perform a k-means clustering using 13 clusters. **In this way, we delineate regions that have similar surface variables, relevant for the glaciers. Furthermore, these regions are also under the influence of similar winds, relevant for the moisture transport.** We performed the clustering with different numbers of clusters and found 13 to give reasonably-sized, yet distinct areas, while also being close to the knee in the total distance away from the cluster means. We perform the tracking on two of these clusters, indicated **later** in Fig. 12, which are close geographically, but have contrasting snowfall trends.

We perform the moisture tracking by releasing moisture parcels from the target area at random positions within the area and advecting them backwards in time using interpolated wind fields on fixed pressure levels. The amount of evaporation A (mm) that contributes to the precipitation in the target area, at a given location x,y and time step t, depends on the evapotranspiration ET (mm), the amount of water in the parcel W_{parcel} (mm), the fraction of water in the parcel that evaporated from the source S_{target}, and the total precipitable water in the column TPW (mm):

$$A_{x,y,t} = \mathrm{ET}_{x,y,t} \frac{W_{parcel,t} S_{target,t}}{\mathrm{TPW}_{x,y,t}} \quad , \qquad (1)$$

The amount of water in the parcel is then updated every time step, including the precipitation P that adds to the parcel when moving back in time.

$$W_{parcel,t-1} = W_{parcel,t} + \left(P_{x,y,t-1} - \mathrm{ET}_{x,y,t-1}\right)\frac{W_{parcel,t}}{TPW_{x,y,t-1}} \quad (2)$$

The fraction **of** precipitation in the target area that originates from a certain source area is then updated as follows:

$$S_{target,t-1} = \frac{S_{target,t}W_{parcel,t} - A_{x,y,t-1}}{W_{parcel,t-1}} \quad (3)$$

We track the parcel until **either more than 99%** of the target precipitation is tracked to a source area, or the tracking time is more than 30 days.

Within the WRF domain, the parcels are advected and the moisture budget is calculated using the WRF wind fields and water fluxes. When a parcel gets within one degree of the edge of the WRF domain, there is a gradual linear change to a use of ERA-Interim reanalysis data to ensure continuous movement of the air parcels over the domain edge. Within one degree distance from the domain edge, the values used to do the moisture tracking are a combination of the WRF and ERA-Interim values: $y_{int} = d*y_{WRF} + (1-d)*y_{ERA}$, where d is the distance to the edge. Outside of the WRF domain, the ERA-Interim values are used.

We noted that the surface moisture flux in ERA-Interim is on average 50% higher than in WRF, resulting in a higher mean and standard deviation of the moisture sources outside the WRF domain. Unfortunately, this systematic offset between the two datasets cannot be easily remediated. Although this will not change the spatial patterns of the moisture source trends in a major way, the absolute values of the trends will be lower in the WRF domain than outside **if there is a scaling factor in moisture flux between the two datasets**. The trends in the Tarim basin will **then** be underestimated with respect to regions such as the Caspian Sea and the Junggar basin.

2.4 Statistics

Pearson correlation coefficients are calculated using the vectors of annual or seasonal mean values. The trends shown in Figs. 2-4, 6, and 14 are the slopes from linear fits to the annual mean vectors.

3. Results

3.1 Validation and comparison

Any attempt to understand the Karakoram anomaly is greatly hampered by the almost complete lack of *in situ* meteorological data in WKSK. The **sparse** weather stations in the region are often situated at relatively low elevation, or in urban

environments, and poorly represent the high mountain climate. Furthermore, different types of precipitation datasets seem to greatly underestimate the precipitation in mountainous terrain (Immerzeel et al., 2015; Ménégoz et al., 2013; Palazzi et al., 2013). These complications imply that any meteorological dataset, including reanalysis datasets, are associated with relatively large fundamental errors in WKSK, which prevents reliable validation of any model of WKSK, such as the one presented in here. **Although not covering the glacierised areas of interest,** we compared our WRF output with data of the region **surrounding** WKSK, to ensure that the WRF output is a reasonable representation of the regional climate between 1980-2010. **Since the glacier model requires annual input, representation of the interannual variability is especially important. Any constant biases are of less importance, since we use relative interannual variations as input for the glacier model. However, biases in temperature will have an effect on the snow-rain partition.**

We collected meteorological station data from **the Global Historical Climatology Network** (GHCN, Lawrimore et al., 2011, accessed June 2019), and selected those that have at least **15** years of full data between 1980-2010. **To be able to compare the WRF output with the station data, we apply a simple downscaling to the WRF temperatures in the grid that includes the station. We fit a linear temperature lapse rate to the temperatures and grid altitudes of a 2x2° box surrounding the station location. We then correct the WRF temperature by applying the lapse rate to the difference in altitude between the WRF grid and the station. Precipitation can also change significantly with location, but there is no clear relation between precipitation and altitude (Bonekamp et al., 2019; Collier and Immerzeel, 2015). For this simple comparison, we do not apply a downscaling of the WRF precipitation.**

Our WRF output produces May-September temperatures that are generally higher than the stations in the Tarim basin. However, biases are generally very low on the Tibetan Plateau, with values around 1°C. The median root-mean-square deviation between WRF and the stations is 1.8°C. The stations generally indicate a strong heating trend. Correlations between the annual variations in annual mean temperatures and mean temperatures between May-September are given in Fig. 2. They show generally very high correlations, with a lowest value of 0.5 (corresponding to $p = 0.005$). This implies that the interannual variability is very well reproduced in WRF. **This is despite the fact that many of these stations are situated in urban environments, with a potential heat island effect, a lack of evaporative cooling that is seen for irrigated agriculture, and a very difference surface energy balance than snow-covered areas. Hence, their locations might not be representative of the wider area, which might give rise to biases and trend differences when comparing the stations to the model outcome.**

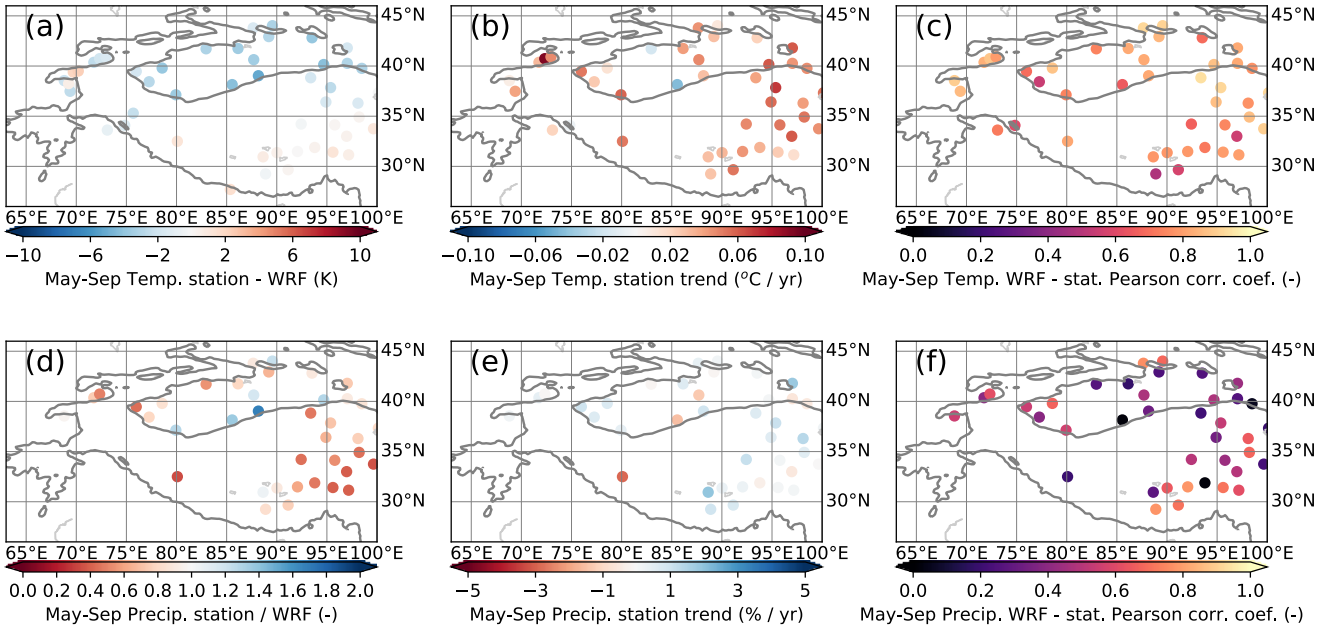

Figure 2: Comparisons between 1980-2010 time series of station data and nearest WRF grid for May-September temperatures (a-c) and May-September precipitation (d-f). Columns show temperature bias (a) and precipitation multiplication factor (d), trends (b,e) and Pearson correlation coefficients. The 2000 m-contour is indicated by a solid line

The stations in Fig. 2 closest to WKSK are almost exclusively in very arid regions, with a significant fraction of snowfall, **which is more difficult to reliably measure than rain (Archer, 1998),** making comparisons of precipitation very uncertain. Fig. 2 shows the **comparison** between time series of May-September precipitation, to limit the effect of snowfall. **Our WRF output is generally wetter than what is measured at the stations, except some locations in the Tarim basin. The median root-mean-square deviation between WRF and the stations is 11.4 mm per month. The stations show that most of the Tarim basin and Tibetan Plateau are seeing an increase in May-September precipitation.** The interannual variations are not represented by WRF as well as they are for temperature, but still show reasonable correlations for most stations, with values around 0.6.

We also compare our WRF simulations with three similar data products with relatively high spatial resolutions, which have recently become available. We do note that all these datasets suffer from the lack of ground truth in WKSK, which means we cannot determine which dataset performs best in this region.

ERA5 is the follow-up of ERA-Interim (Copernicus Climate Change Service, 2017), with an improved spatial resolution of 0.25°, an improved temporal resolution, a more appropriate model input for e.g. sea surface temperatures, and more assimilated data. ERA5-Land is atmospherically forced by ERA5, and provides an even higher spatial resolution (0.1°)

for land surface properties (Copernicus Climate Change Service (C3S), 2019). Finally, we include the HAR dataset with a resolution of 10 x 10 km, which uses WRF to downscale the NCEP FNR reanalysis dataset and re-initialises every day (Maussion et al., 2014). We compare temperatures between May-September, and annual precipitation, which give an indication of the parameters that are most relevant for glacier mass balance modelling. Because of the limited time overlap between the different datasets, we could only fully compare the period 2001-2010.

We binned all data to the same 0.5° x 0.5° grid to allow direct comparison. The mean values, trends, and interannual variability are compared in Figs. 3 and 4. It shows that ERA5 and ERA5-Land are nearly identical, and we only refer to ERA5 below. Our WRF model yields a warmer Karakoram than the other three datasets. Generally, the mean temperature differences are relatively minor, except for a warmer Tarim basin compared to HAR. We find very similar temperature trends as ERA5, although with smaller magnitudes. The magnitudes of the trends are also generally smaller than those in the station data (Fig. 2). The WRF interannual temperature variations correlate very well with ERA5, except two areas in the Tarim and the inner Tibetan Plateau. This is not surprising, given that our WRF model is forced by the similar ERA-Interim data. The whole western part of HMA, including WKSK, is especially well-correlated to ERA5. In that region, the correlation with HAR is weaker, but the correlation between HAR and our WRF data is very strong in East HMA. The differences with HAR might be explained by the different forcing, or by the difference in used physics modules, but this requires further study.

Differences between datasets are larger for precipitation, at least for the mean values and interannual variability. Our WRF simulations give results that are relatively wet in the Karakoram, and relatively dry in the Himalaya. However, the precipitation trends are very similar to ERA5 in both pattern and magnitude. An exception is the arid Tarim basin, which has an increasing trend in WRF, but a decreasing trend in ERA5. HAR shows a positive precipitation trend in most of HMA, with a very high trend in the Tarim basin. The correlation of the interannual variability is low in WKSK and parts of Tien Shan, which could be explained by the relatively high influence of the irrigated areas in the Tarim basin on the annual precipitation (de Kok et al., 2018, Fig. 3). Since our WRF model outcome is the only one of the four datasets that explicitly includes irrigation, this could explain the difference in annual variability.

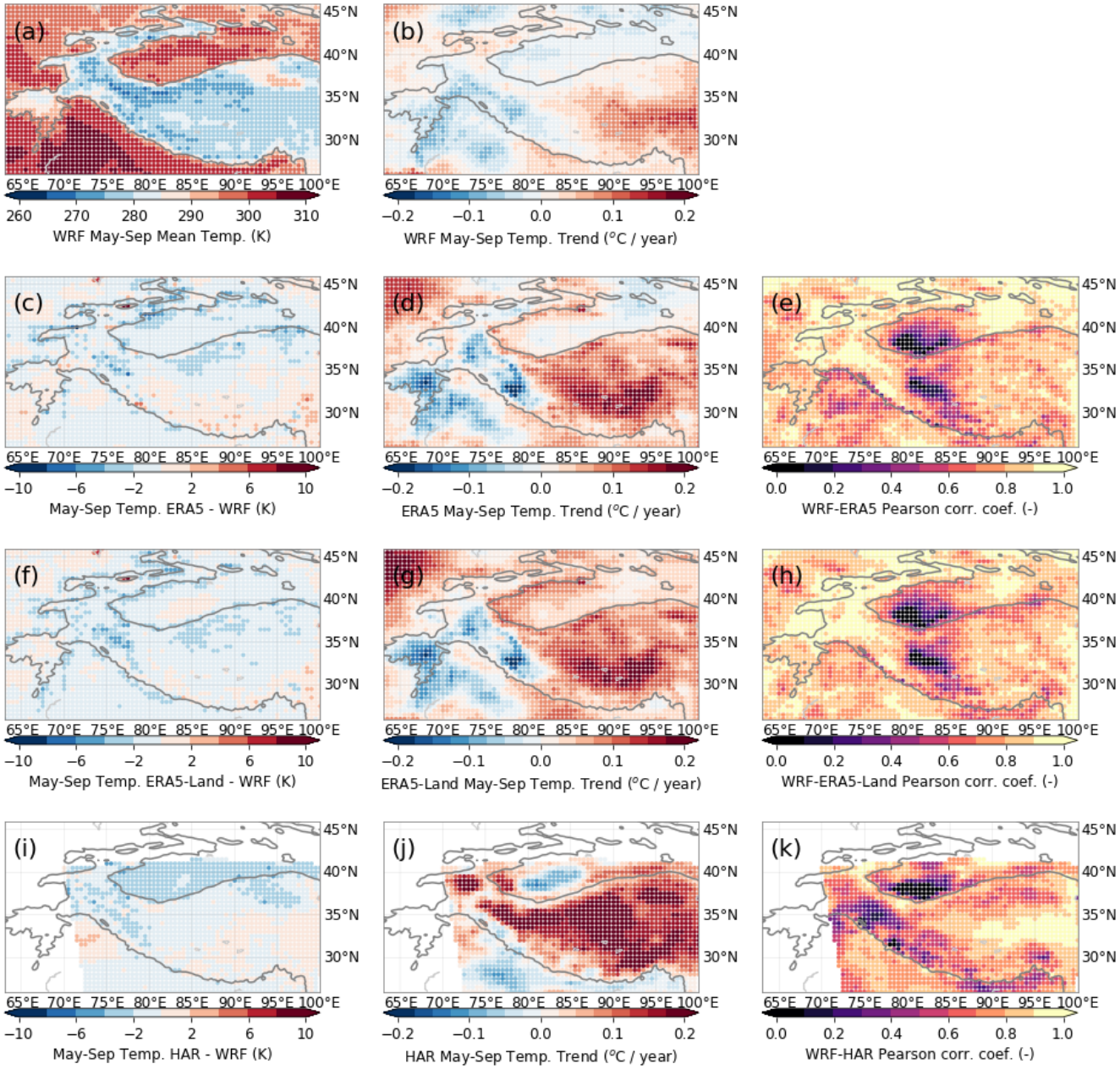

Figure 3: Comparison of WRF temperature output [a-b] with three other datasets (ERA5 [c-e], ERA5-Land [f-h], and HAR [i-k]). Columns show biases (c,f,i) with respect to the May-September mean temperature (a), May-September temperature trends (b,d,g,j), and Pearson correlation coefficients between the datasets and our WRF results (e,h,k). The 2000 m elevation contour is indicated by a solid line.

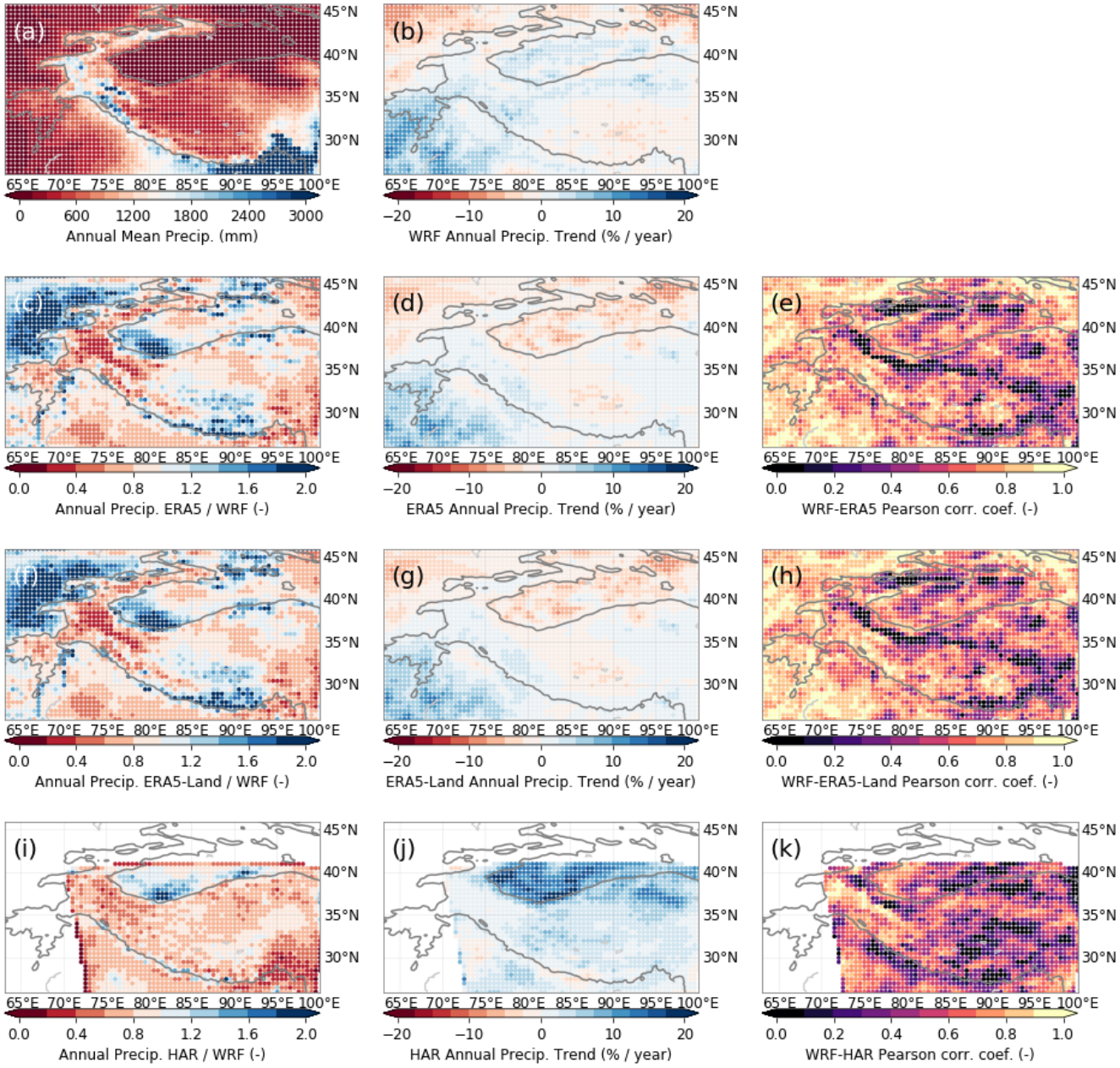

Figure 4: Comparison of WRF precipitation output [a-b] with three other datasets (ERA5 [c-e], ERA5-Land [f-h], and HAR [i-k]). Columns show precipitation multiplication factors (c,f,i) with respect to the annual mean precipitation (a), annual precipitation trends (b,d,g,j), and Pearson correlation coefficients between the datasets and our WRF results (e,h,k). The 2000 m elevation contour is indicated by a solid line.

Another **variable** that is important in our model is evapotranspiration. It cannot be directly measured remotely, but there are several datasets that calculate it from other remotely sensed products, either directly or through data assimilation. These datasets vary greatly, as we illustrate in Fig. 5 for July 2010. We show evapotranspiration from GLEAM v 3.3a (Martens et al., 2017; Miralles et al., 2010), which assimilates various soil moisture, temperature, radiation, and precipitation products. Furthermore, we show SSEBop (Senay, 2018) data, which uses MODIS temperatures directly, ERA-Interim reanalysis data, and our WRF output. On the inner Tibetan Plateau, the WRF output agrees very well with the GLEAM data. Interannual variations also match very well between WRF and GLEAM in snow-free areas on the Tibetan Plateau, with correlation coefficients above 0.5 for time series between 1980-2010. However, it is clear that GLEAM does not represent the irrigated areas well, with unrealistically low evapotranspiration in heavily irrigated arid regions in July. In contrast, SSEBop shows very high evapotranspiration in the irrigated regions. The WRF output better resembles SSEBOP in those areas, although generally has lower **maxima**, which are only in part explained by the difference in spatial resolution, **as is evident from e.g. averaging over 1x1° areas**. ERA-Interim does not show the irrigation as prominently as WRF or SSEBop, but has a generally higher evapotranspiration values over unirrigated areas, such as the Tibetan Plateau. In general, the WRF simulated evapotranspiration is intermediate compared to the other datasets with plausible spatial patterns and magnitudes.

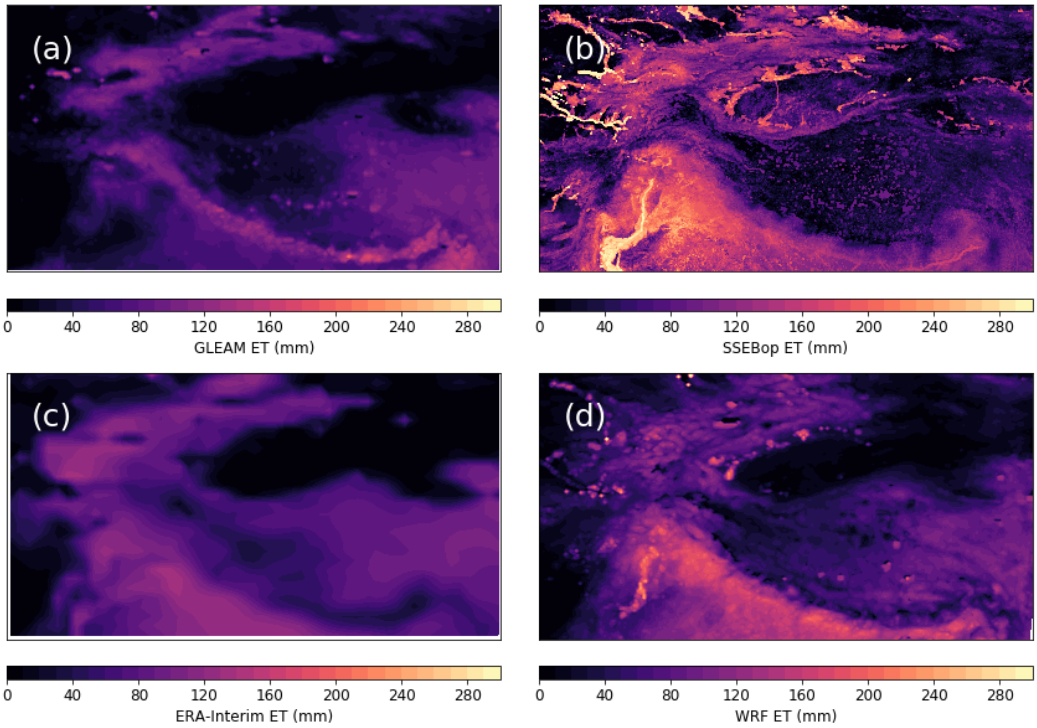

765 **Figure 5: Evapotranspiration for July 2010 from GLEAM (a), SSEBop (b), ERA-Interim (c), and WRF (d). Mean values for the plotted domains are: 44 mm (a), 46 mm (b), 57 mm (c), and 59 mm (d).**

3.2 Climatic trends

To get an impression how glaciers might have been affected by changes in the climate, we illustrate the trends for two relevant variables: the 2m-temperature in the melt season and the annual snowfall (Fig. 6, see also Fig. 7 for representative time series).
770 For each grid point, the melt season was defined as the months where the mean daily temperature is above -5 °C, since for these months temperatures will likely be above freezing at least part of the time. A threshold value of 0 °C slightly increased the positive temperature trends at lower elevations in WKSK, but meant no trends for the highest elevations could be determined. The trends show that temperatures in the melt season have generally increased, with the northern part of the domain heating up the fastest and parts of the Indo-Gangetic Plain, Kunlun Shan, Karakoram, and the Tibetan Plateau showing
775 only modest increases in temperature. **Fig. 7 shows that the trend and the interannual variability of temperature are very similar for nearby regions of both growing and shrinking glaciers.** The snowfall trends **in Fig. 6** have a very different pattern, with most of the Tibetan Plateau showing an increase and the western and southern mountain ranges, such as the Himalaya and the Hindu-Kush, showing a decrease in snowfall. **Furthermore, the mean level, the trend, and the**

interannual variability of snowfall is quite distinct for the two nearby regions of contrasting glacier mass balance trends. The increase in snowfall in WKSK mainly occurs in May, June, and September, whereas the decrease of snowfall in southwestern HMA occurs mainly in March (see Fig. 8 for region averages).

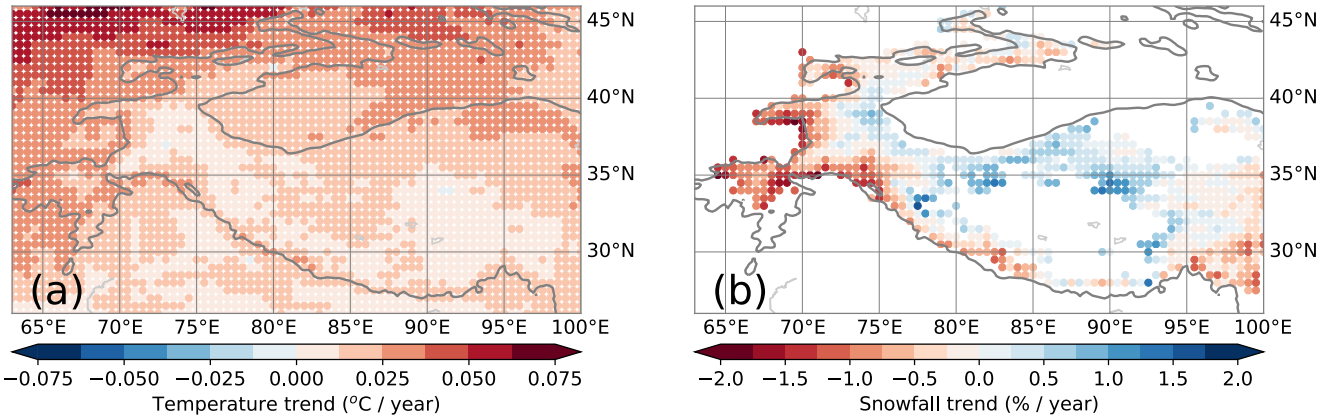

Figure 6: Trends between 1980-2010 of temperature in the melt season (a) and annual **snowfall (b), averaged over 0.5x0.5° bins for clarity. Regions with monthly snowfall of less than 10 mm were masked out. The 2000 m elevation contour is indicated by a solid line.**

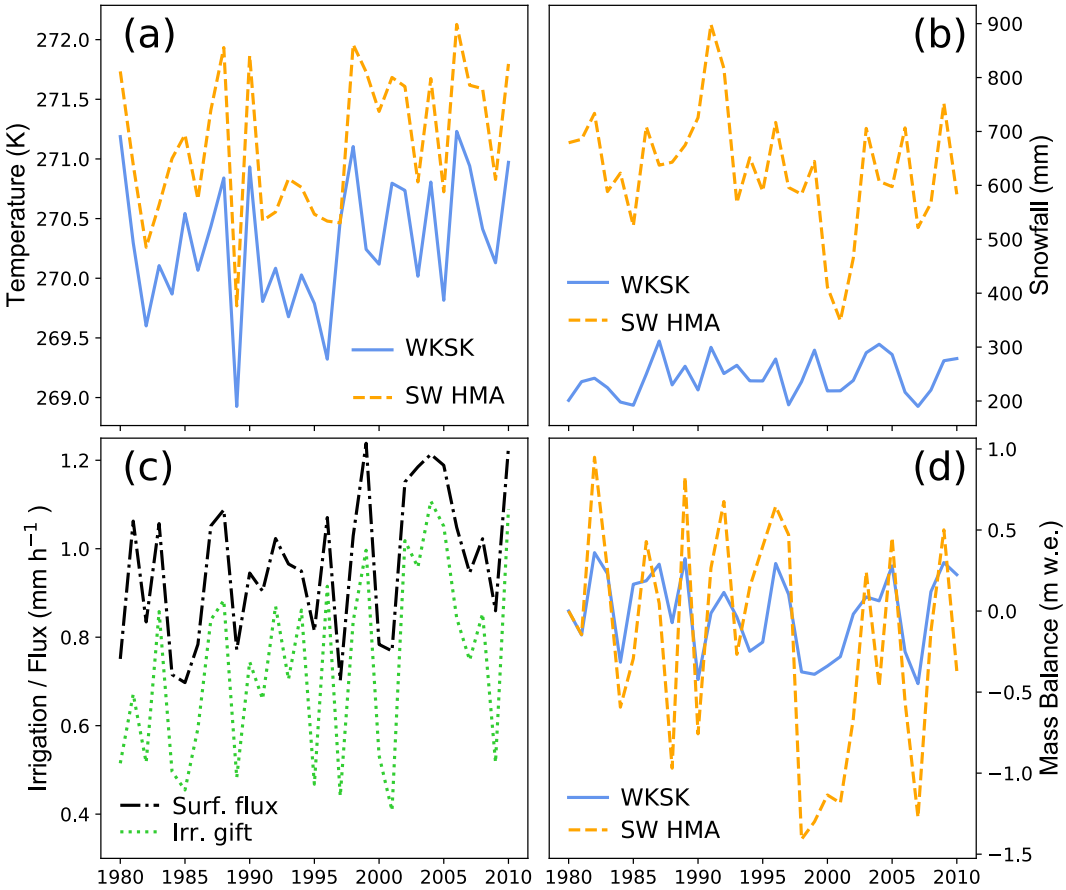

Figure 7: Time series of annual mean temperature (a), annual **snowfall (b), mass balance (d)** for two nearby 2x3° bins that have, on average, growing glaciers (38-40° N, 73-76° E, blue lines) and shrinking glaciers (35-37° N, 72-75° E, orange, dashed lines). **Panel *c* shows the time series of annual irrigation gift (green, dotted line) and annual surface moisture flux (black, dot-dashed line) for the most heavily irrigated point in the Tarim.**

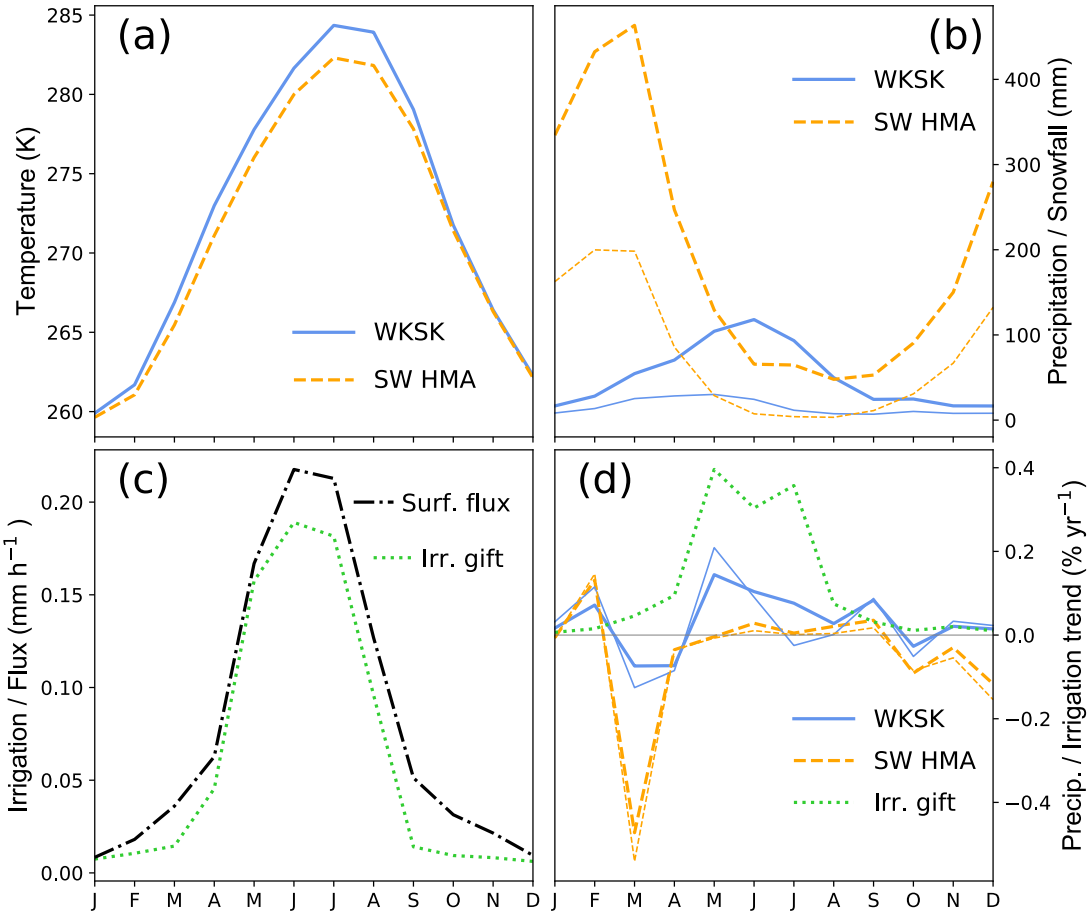

Figure 8: a) Mean seasonal cycle of temperature and b) precipitation (thick lines) and snowfall (thin **lines) between 1980-2010 for the WKSK (blue lines) and southwestern HMA (orange, dashed lines), as shown in Fig. 11b,d. c) Mean seasonal cycle of the irrigation gift (green, dotted line) and surface moisture flux (black, dot-dashed line) of the most heavily irrigated point in the Tarim. d) Trends in precipitation (thick lines) and snowfall (thin lines) for the WKSK (blue lines) and southwestern HMA (orange, dashed lines), and the trend in irrigation from the most heavily irrigated point in the Tarim (green, dotted line), all as percentages of the annual mean value.**

3.3 Glacier mass balances

The resulting pattern of simulated mass balance (Fig. 9) shows a strong resemblance to the measured pattern of mass balances of recent decades. Most notably, we also obtain growing glaciers in WKSK, whereas the glaciers in other regions show large mass losses. In fact, all points where we model glacier growth in Fig. 9a also show growth or stable conditions in observations (Brun et al., 2017; Kääb et al., 2015), except one point in Kääb et al., (2015). A more detailed quantitative comparison of the above results and the observed mass balances is hampered by the fact that our simulations only go out to 2010, **and hence we cannot compare with the most recent, and most accurate geodetic mass balance data. However,** we compare our results for the **intermediate** period 2000-2008, **as presented by Brun et al. (2017),** in Fig. 10. The results generally match reasonably

well, although our model seems to show too little growth for the growing glaciers. However, note that the errors on these observations (Brun et al., 2017) are large (~0.3 m w.e.). Furthermore, both the climate model and the glacier model will be associated with errors. **However, in both cases the growing glaciers are only present in the same region, mainly WKSK and the Tibetan Plateau.** By modulating the initial mass balance in the model, we find that on average 41% of the modelled mass balance in 2010 is determined by the initial mass balance in 1980. Although the mass balances in 1980 were observed to be less extreme than in the 21st century (Bolch et al., 2012; Maurer et al., 2019), parts of HMA already had negative mass balances then, with the magnitude of initial mass balances generally less than 0.4 m w.e. yr^{-1}. This would result in an error on the mass balances in Fig. 8 of less than 0.2 m w.e. yr^{-1}. Despite these uncertainties, our results clearly show that the climatic change of the recent decades has favoured growth of the glaciers in the regions where actual growth is observed, and not in the places where glaciers are melting fastest.

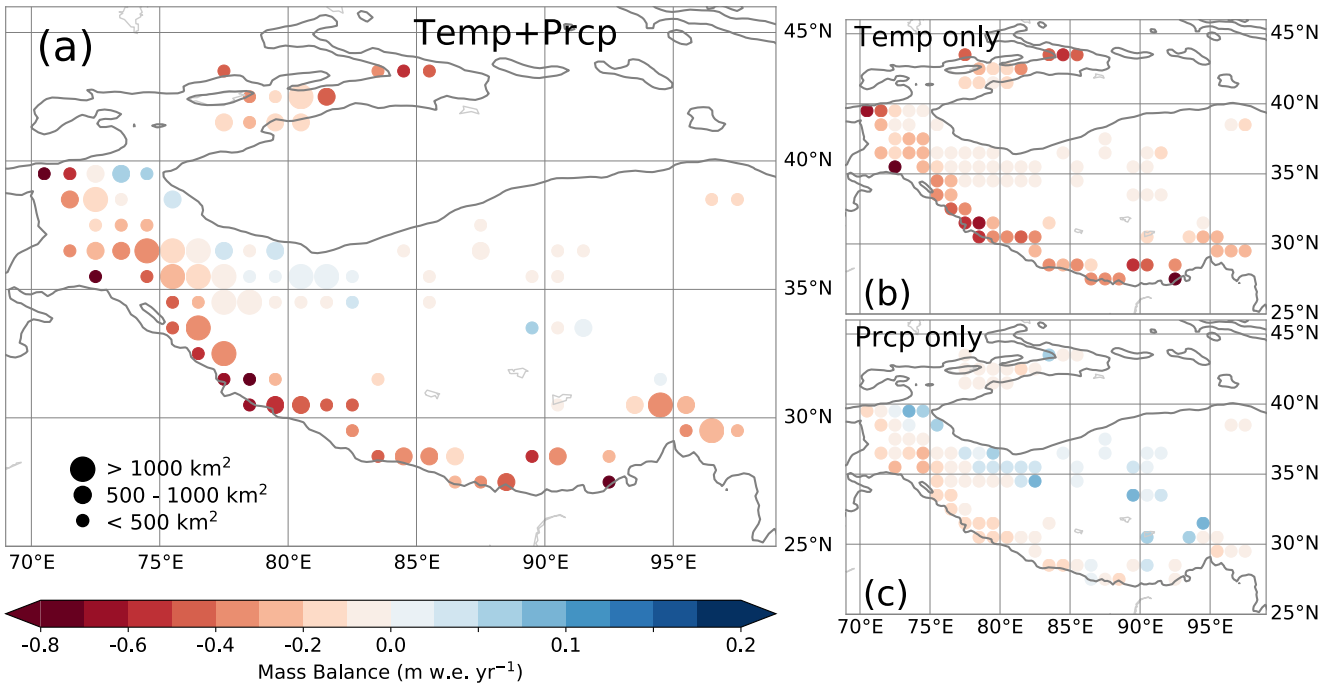

Figure 9: Simulated mean mass balance between 2000-2010 forced by changes in temperature and annual **snowfall from WRF (a), only changes in temperature from WRF (b), and only changes in** annual **snowfall from WRF (c). Results are binned in 1x1° bins, and bins with total glacier volumes less than 5 km^3 are not shown, to enable comparison with previous studies. The 2000 m elevation contour is indicated by a solid line.**

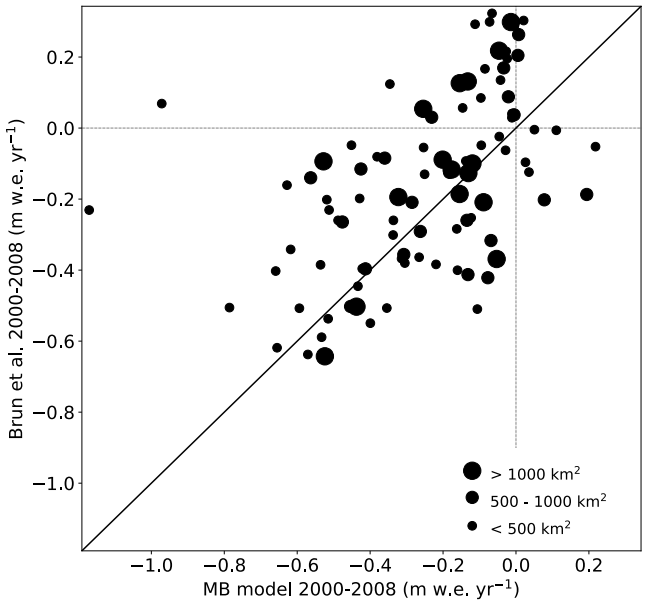

Figure 10: Comparison between mean modelled mass balances from this work, binned on a 1x1° grid as in Fig. 9, and those derived from observations of Brun et al. (2017), which are on the same grid, between 2000-2008.

We also ran the glacier mass balance model forced by changes in temperature or snowfall only, to disentangle the model sensitivities of the two different variables on the glacier mass balances (Figures 9b and 9c). These results show that the glaciers in the western and southern HMA mainly lose mass due to the increase in temperature, **while the decrease in precipitation gives a much smaller mass balance response in this region**. On the other hand, in the regions where the glaciers are growing, the glaciers are barely affected by the temperature increases in our model. The glacier growth in these regions is mainly caused by an increase in snow (Fig. 9c). Furthermore, the increase in snow is possibly also responsible for moderating the temperature increases due to the high albedo of fresh snow, which leads to less energy being used for melt. However, the weak temperature response in WKSK is not only caused by the limited temperature trends, but is also due to the limited glacier temperature sensitivity there. We demonstrate this by forcing the glacier model with uniform temperature and precipitation trends (Fig. 11). The reduced temperature sensitivity is in line with previous work (Sakai and Fujita, 2017; Wang, et al., 2019), **which argue that the generally large masses of the glaciers, and high equilibrium line altitudes, are important in explaining the lower temperature sensitivity in WKSK**. The decrease in snowfall in the western and southern HMA has a far smaller impact on the mass balance than the increase in temperature. Especially the Himalaya show a low sensitivity to precipitation (Fig. 11). To be able to model thousands of glaciers, our mass balance model is relatively simple and does not solve the full energy balance. A full energy balance model at 1 km resolution has shown that the temperature increases can amplify melt in the monsoon-dominated Himalaya, whereas snowfall increases in the melt season can amplify glacier growth in the Karakoram (Bonekamp et al., 2019). Hence, more detailed models will likely strengthen our conclusion that the observed mass gains are

caused by snow increases, whereas the observed mass losses are mainly caused by temperature increases. Unfortunately, modelling the climate and glaciers of the entire HMA at a sub-kilometre resolution for 30 years is currently beyond our capabilities.

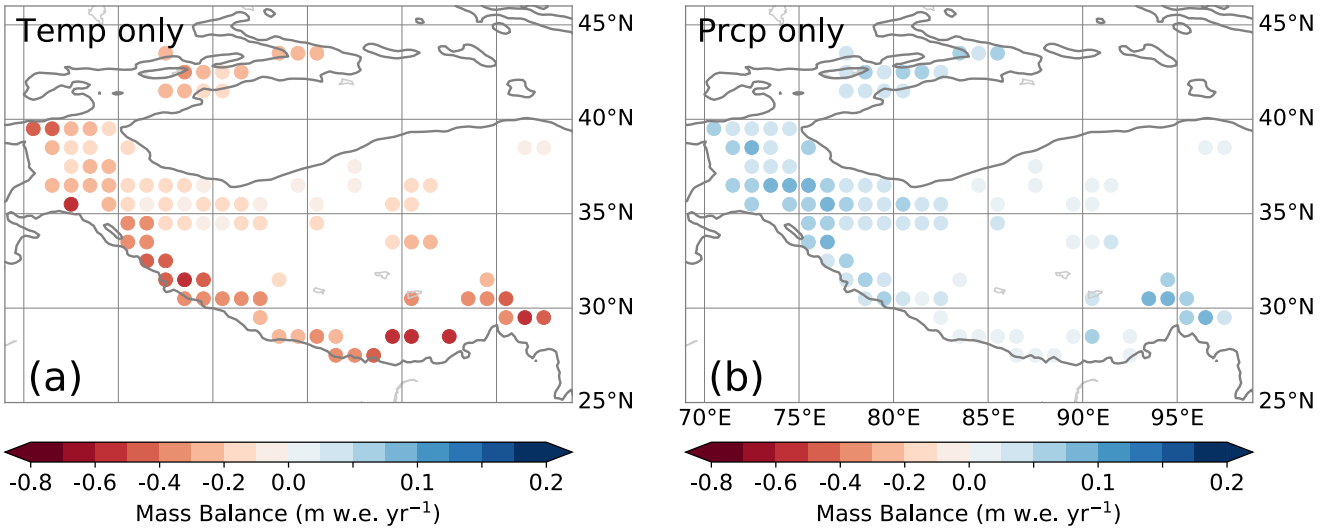

Figure 11: Simulated mean mass balance between 2000-2010 forced by a spatially uniform and constant temperature increase of +0.01 °C yr^{-1}, with snowfall kept constant (a), and a spatially uniform and constant snowfall increase of +0.5% yr^{-1} of the annual mean value, with temperature kept constant **(b). Panels *a* and *b* thus show the relative sensitivity to temperature and snowfall, respectively.**

3.4 Moisture sources

The trends in moisture source regions for WKSK (Fig. 12a,b) indicate that the largest increases in moisture from a given source to precipitation in WKSK occur in the mountains themselves. This increase in recycling occurs mainly in May, and is also the main cause of the increase in precipitation in September (see Fig. 13). The increase in recycling is probably a natural consequence of the increased precipitation there. The regions with the second largest increases are the areas in the Tarim basin **where irrigation has increased the most**, which contributes mainly in May-July, **with May showing the largest resulting increase in snowfall** (see Figs. 8 and 13). In July, the increase in Tarim irrigation still contributes to increasing precipitation in WKSK, but it falls more in the form of rain, compared to May, where it is mainly snow (Fig. 8). Another region that contributes to the increase in precipitation in WKSK is the Junggar basin, northeast of the Tarim basin. This is another arid region that has experienced rapid increases in irrigation. The increases per grid point are lower there, but spread out over a larger area. A final source region with an overall large positive trend is the Caspian Sea and the Caucasus. Note again that, due to a systematic offset in surface moisture flux between WRF and ERA-Interim, the moisture source trends in the Tarim and HMA are underestimated with respect to the other regions.

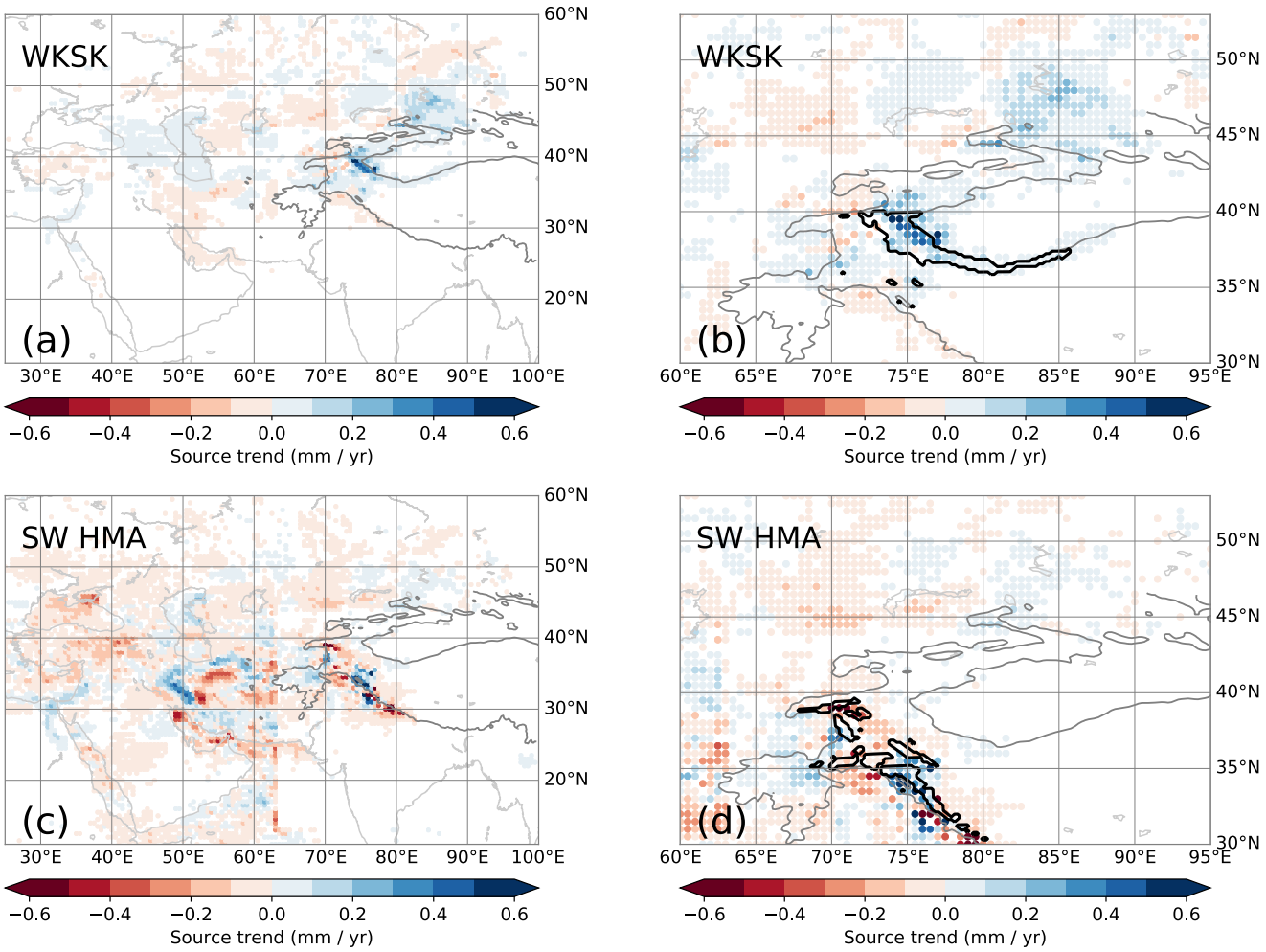

Figure 12: Trends in the amount of moisture from a given source contributing to precipitation trends in the target area (a,c), with a detailed view (b,d) around the target area from which the parcels were released (contoured in bold) for WKSK (a,b) and southwestern HMA (c,d). Trends with absolute magnitudes smaller than 0.02 mm yr^{-1} are made white. The 2000 m elevation contour in the WRF domain is indicated by a solid line.

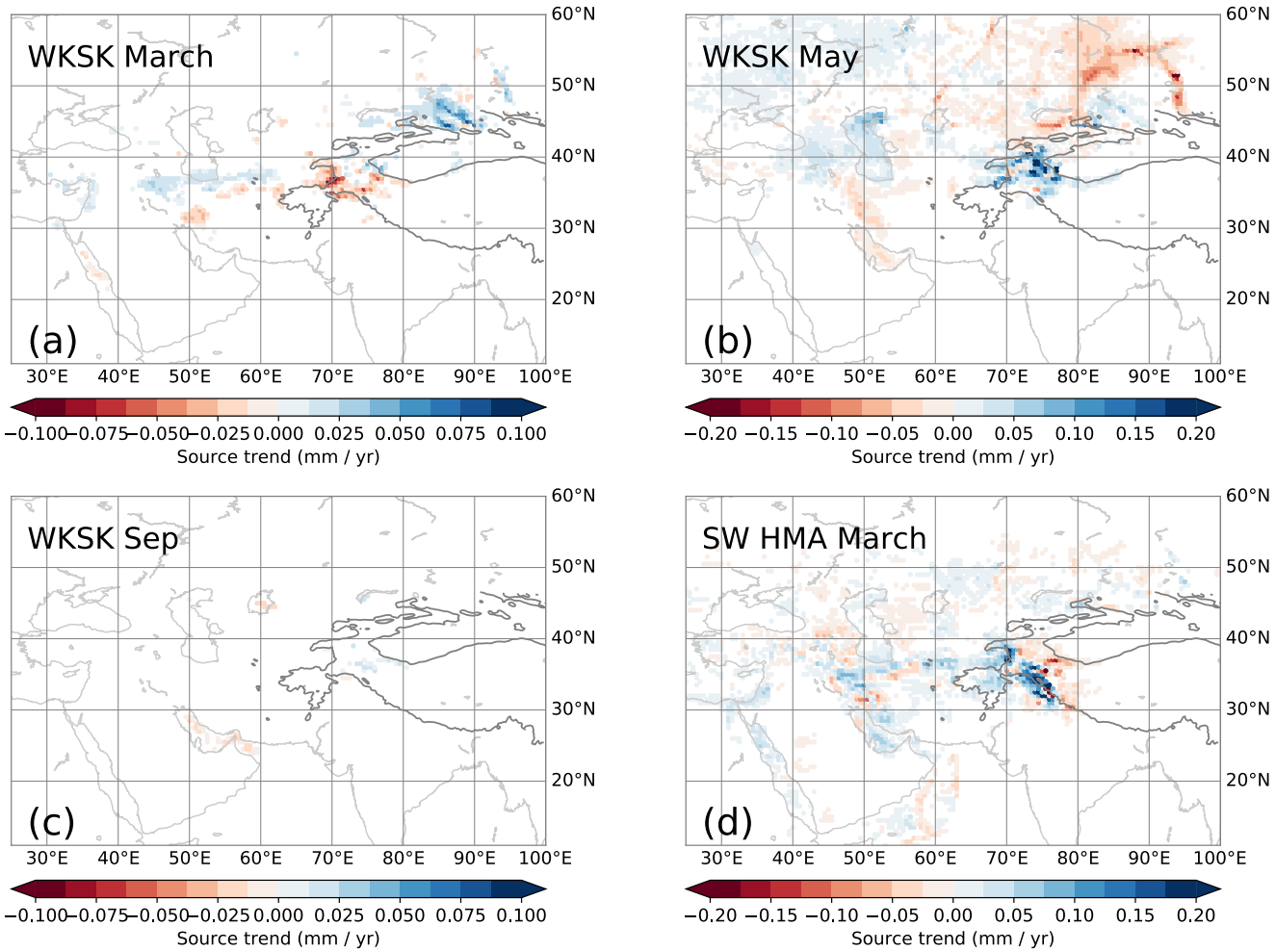

Figure 13: Trends in the amount of moisture from a given source for WKSK for March (a), May (b), September (c) and for southwestern HMA in March (d). These months correspond to large negative or positive trends in snowfall in Fig. 8. Note the different scales.

These results imply that evapotranspiration from irrigated areas in arid Northwest China play a large role in adding water to parts of HMA and hence to the observed positive mass balances. This is in line with recent work that shows that the recent wetting of Central Asia and the Tarim basin is associated with an increase in evapotranspiration in these regions (Dong et al., 2018; Peng et al., 2018; Peng and Zhou, 2017). The increase in the total evapotranspiration is influenced by the increase in potential evapotranspiration (Fang et al., 2018), increase in water availability (Jian et al., 2018), and increase in irrigated land area. On the interannual timescale, precipitation in WKSK strongly correlates with the moisture source amount in the western Tarim basin (Pearson r=0.96 below 3500 m, r=0.68 for the entire WKSK, as indicated in Fig. 12b). A similar correlation exists between the WKSK precipitation and the Caspian Sea moisture source amount (r=0.89 below 3500 m, r=0.43 for the entire

WKSK), showing the importance of the large-scale weather patterns. For the Junggar basin, this correlation is weaker (r=0.65 below 3500 m, r=-0.14 for the entire WKSK), since this region contributes **relatively more** in winter (Fig. 13)**, when less snowfall reaches WKSK (Fig. 8)**.

When performing the moisture tracking for the southwestern part of HMA, where snowfall has generally decreased (Fig. 12c,d), also the Caspian Sea and the Junggar basin positively contribute to the snowfall trend, whereas for these ranges the Tarim basin does not contribute to the snowfall trend, with maximal trends in moisture sources of less than 0.1 mm yr^{-1}. These results show that the irrigated areas in the Tarim basin are especially important in influencing the moisture supply to the Western Kunlun Shan (de Kok et al., 2018).

4. Conclusion and discussion

Our simulations, based on ERA-Interim and GLDAS reanalysis data, indicate that an increase of snowfall and a low temperature sensitivity are the main reasons why glaciers are growing or stable in western Kunlun Shan and Karakoram. This is the first time that the observed pattern of glacier mass balances in HMA is reproduced in a consistent way. **Our snowfall trends between 1980-2010 show some similarities, but also major differences with respect to a similar WRF study that did not include irrigation and used another re-analysis dataset (Norris et al., 2018). For instance, our temperature trends do not exhibit the strong summer cooling at low altitudes (e.g. the Tarim basin), and are more in line with station data** (Waqas and Athar, 2018; Xu et al., 2010) **in that respect. However, contrasting precipitation trends in WKSK and southwestern HMA, similar to Fig. 6, are also present in ERA5 data and the Norris et al. study (see Farinotti et al., 2020) Although the interannual variability of temperature and precipitation is reasonably reproduced, and our precipitation trends are similar to those in other datasets, our model results are associated with uncertainties, which are partly irreconcilable due to a lack of *in situ* measurements in WKSK.** Furthermore, different parameterisations in the regional climate model, different irrigation schemes, and different glacier models will likely yield slightly different results. Using an ensemble of such approaches could be used to assess the robustness of the results presented here in the future. Furthermore, detailed studies at smaller scales will give more insight into individual glacier behaviour.

The pattern of precipitation trends in Fig. 6b roughly matches the pattern that is expected from an increasing influence of summer westerlies, as shown by Mölg et al. (2017). These westerlies are also associated with strong heating and drying trends of the Indus Basin. An increase in irrigation also produces a very similar precipitation pattern, yet causes a cooling and wetting of the Indus Basin (de Kok et al., 2018). Our JAS trends of near-surface temperature and specific humidity (Fig. 14) indicate mostly cooling and wetting trends, which is more in line with the increase in irrigation than with the increase in summer westerlies. ERA5 data for JJA also indicates a similarly strong irrigation effect in the Indus basin (Farinotti et al., 2020). The moisture tracking results (Figs. 12 and 13) indicate that much of the additional

snowfall occurs in spring and summer, and originates from the East, with a large role for the irrigated areas. However, the May westerlies clearly have an important role in transporting the increase in evaporation from the Caspian Sea (Chen et al., 2017) to WKSK. Besides the Caspian Sea, the westerlies are mainly associated with a decrease in snowfall when the whole year is considered (Fig. 12a). The pattern of precipitation trends in Fig. 5b is not only the result of changes in summer. The decrease in precipitation in southwestern HMA is also clearly associated with westerly winds in winter, but not those in summer (see Figs. 8d and 12c).

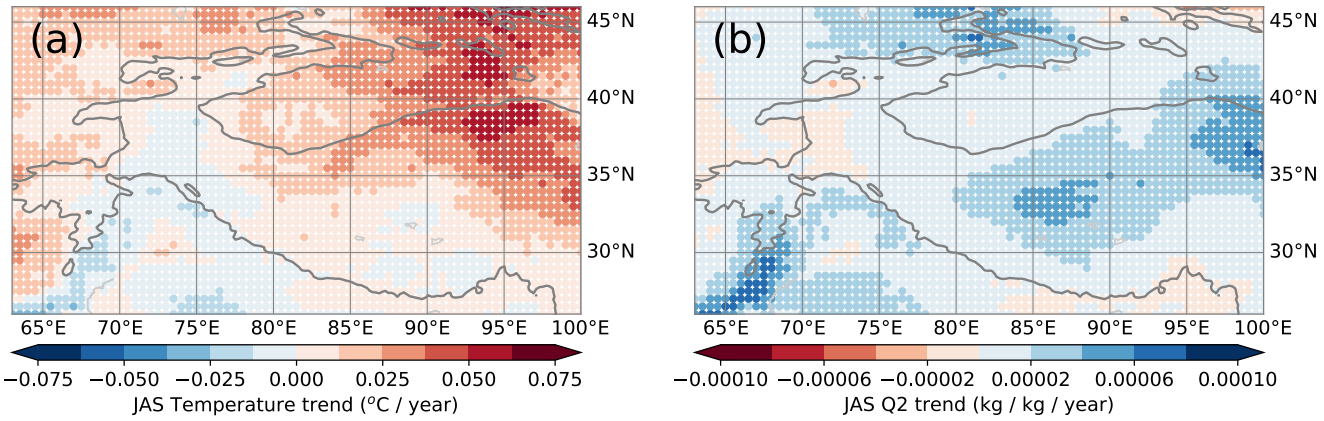

Figure 14: Trends between 1980-2010 of near-surface temperature (a) and specific humidity (b) between July-September, averaged over 0.5x0.5° bins for clarity. The 2000 m elevation contour is indicated by a solid line.

We show that the growing irrigated area in the arid region of Northwest China plays an important role in the increase in snowfall in WKSK. Previous studies have already shown that increases of irrigation in Northwest China can add precipitation to neighbouring mountains (Cai et al., 2019; de Kok et al., 2018), but we now show this process of increasing irrigation is also important compared to other changes in the atmosphere over the last few decades. Already before 1980, irrigation has increased in Northwest China (Fang et al., 2018), possibly contributing to the stable glacier conditions then. Future evolution of snowfall in this part of HMA is partly linked to how the irrigated areas develop in the future. Changes in temperature, irrigated area, or irrigation efficiency are therefore important parameters in understanding future run-off from glaciers and snow in WKSK. The increase in water availability for irrigation in Northwest China might be partly the result of the loss of glacier mass in Tien Shan (Dong et al., 2018). The mass loss will first result in an increase in glacier melt run-off into the Tarim basin, but ultimately the run-off will decrease as the glaciers shrink to a small size (Kraaijenbrink et al., 2017). On the other hand, if the primary source of irrigation water is groundwater, the amount of irrigation for the region will also have a limited sustainable or economic level. Once the groundwater is depleted, **our results suggest that** the glaciers in WKSK will also receive less snowfall from this region, resulting in their retreat. The relative importance of groundwater extraction, melt from Tien Shan, and recycling from WKSK, for water availability in the Tarim is yet unknown and will require future study. Furthermore,

improving the estimates of irrigation gifts, e.g. by remote sensing, could also improve the past climate reconstruction of WKSK. Greening and warming in West-Asia could provide additional snowfall to WKSK, together with an increase in westerly disturbances (Cannon et al., 2015; Kapnick et al., 2014), but if temperatures in HMA keep increasing, the increase in melt will probably counteract glacier growth in most of HMA in the long term. It is clear that the coupling between glacier mass balance, runoff, and irrigation in different regions creates a complex problem of water availability, which will need to be researched further to inform decision makers on irrigation policies.

Acknowledgements

We acknowledge funding from the European Research Council (ERC) under the European Union's Horizon 2020 research and innovation program (grant number 676819), the Netherlands Organisation for Scientific Research Innovational Research Incentives Schemes VIDI and VENI (016.181.308 and 016.171.019), and the Strategic Priority Research Program of Chinese Academy of Sciences (grant number. XDA20100300). Computing time was provided by the SURFsara CARTESIUS National Supercomputer of the Netherlands Organization for Scientific Research. We thank Rens van Beek for distribution of the PCR-GLOBWB irrigation data. We thank Fanny Brun and Jesse Norris for discussion. **We thank Thomas Mölg, Dieter Scherer, and an anonymous reviewer for their careful reading and useful comments, which improved the manuscript.**

Code and data availability

The data underlying our results in Figs. 6-14, i.e. monthly mean output from WRF of temperature and precipitation, annual glacier mass balances, and annual moisture sources, will be directly accessible at *dataverse.nl (*https://hdl.handle.net/10411/ATONZD). Other data is available from the authors upon request. WRF and the glacier mass balance model are freely available. The moisture tracking model is available upon request from Obbe A. Tuinenburg.

Author contributions

R.J.d.K. and W.W.I. designed the study, with input from all authors. R.J.d.K. performed the WRF modelling, P.D.A.K. performed the glacier mass balance modelling, and O.A.T. performed the moisture tracking. All authors contributed to the writing and editing of the manuscript.

Competing interests

The authors declare that they have no conflict of interest.

References

Archer, D.: Snow measurement, in Encyclopedia of Hydrology and Lakes. Encyclopedia of Earth Science., Springer, Dordrecht., 1998.

van Beek, L. P. H. and Bierkens, M. F. P.: The Global Hydrological Model PCR-GLOBWB: Conceptualization, Parameterization and Verification, Utr. Univ. Dep. Phys. Geogr. http//vanbeek.geo.uu.nl/suppinfo/vanbeekbierkens2009.pdf [online] Available from: http://vanbeek.geo.uu.nl/suppinfo/vanbeekbierkens2009.pdf, 2008.

van Beek, L. P. H., Wada, Y. and Bierkens, M. F. P.: Global monthly water stress: 1. Water balance and water availability, Water Resour. Res., 47(7), doi:10.1029/2010WR009791, 2011.

Beljaars, A. C. M.: The parametrization of surface fluxes in large???scale models under free convection, Q. J. R. Meteorol. Soc., 121(522), 255–270, doi:10.1002/qj.49712152203, 1995.

Bocchiola, D. and Diolaiuti, G.: Recent (1980-2009) evidence of climate change in the upper Karakoram, Pakistan, Theor. Appl. Climatol., 113(3–4), 611–641, doi:10.1007/s00704-012-0803-y, 2013.

Bolch, T., Kulkarni, a., Kaab, a., Huggel, C., Paul, F., Cogley, J. G., Frey, H., Kargel, J. S., Fujita, K., Scheel, M., Bajracharya, S. and Stoffel, M.: The State and Fate of Himalayan Glaciers, Science (80-.)., 336(6079), 310–314, doi:10.1126/science.1215828, 2012.

Bonekamp, P., de Kok, R., Collier, E. and Immerzeel, W.: Contrasting meteorological drivers of the glacier mass balance between the Karakoram and central Himalaya, Front. Earth Sci., in press, doi:doi: 10.3389/feart.2019.00107, 2019.

Brun, F., Berthier, E., Wagnon, P., Kääb, A. and Treichler, D.: A spatially resolved estimate of High Mountain Asia glacier mass balances from 2000 to 2016, Nat. Geosci., 10(9), 668–673, doi:10.1038/ngeo2999, 2017.

Cai, P., Luo, G., He, H., Zhang, M. and Termonia, P.: Agriculture intensification increases summer precipitation in Tianshan, Atmos. Res., 227(April), 140–146, doi:10.1016/j.atmosres.2019.05.005, 2019.

Cannon, F., Carvalho, L. M. V., Jones, C. and Bookhagen, B.: Multi-annual variations in winter westerly disturbance activity affecting the Himalaya, Clim. Dyn., 44(1–2), 441–455, doi:10.1007/s00382-014-2248-8, 2015.

Chen, J. L., Pekker, T., Wilson, C. R., Tapley, B. D., Kostianoy, A. G., Cretaux, J. F. and Safarov, E. S.: Long-term Caspian Sea level change, Geophys. Res. Lett., 44(13), 6993–7001, doi:10.1002/2017GL073958, 2017.

Collier, E. and Immerzeel, W. W.: High-resolution modeling of atmospheric dynamics in the Nepalese Himalayas, J. Geophys. Res. Atmos., 120, 98822–9896, doi:10.1002/2015JD023266, 2015.

Cook, B. I., Shukla, S. P., Puma, M. J. and Nazarenko, L. S.: Irrigation as an historical climate forcing, Clim. Dyn., 44(5–6), 1715–1730, doi:10.1007/s00382-014-2204-7, 2015.

Copernicus Climate Change Service: ERA5: Fifth generation of ECMWF atmospheric reanalyses of the global climate, Copernicus Clim. Chang. Serv. Clim. Data Store [online] Available from: https://cds.climate.copernicus.eu/cdsapp#!/home (Accessed 20 December 2019), 2017.

Copernicus Climate Change Service (C3S): C3S ERA5-Land reanalysis, Copernicus Clim. Chang. Serv. Clim. Data Store [online] Available from: https://cds.climate.copernicus.eu/cdsapp#!/home (Accessed 5 January 2020), 2019.

Dee, D. P., Uppala, S. M., Simmons, A. J., Berrisford, P., Poli, P., Kobayashi, S., Andrae, U., Balmaseda, M. A., Balsamo, G., Bauer, P., Bechtold, P., Beljaars, A. C. M., van de Berg, L., Bidlot, J., Bormann, N., Delsol, C., Dragani, R., Fuentes, M., Geer, A. J., Haimberger, L., Healy, S. B., Hersbach, H., H??lm, E. V., Isaksen, L., K??llberg, P., K??hler, M., Matricardi, M., Mcnally, A. P., Monge-Sanz, B. M., Morcrette, J. J., Park, B. K., Peubey, C., de Rosnay, P., Tavolato, C., Th??paut, J. N. and Vitart, F.: The ERA-Interim reanalysis: Configuration and performance of the data assimilation system, Q. J. R. Meteorol. Soc., 137(656), 553–597, doi:10.1002/qj.828, 2011.

Dehecq, A., Gourmelen, N., Gardner, A. S., Brun, F., Goldberg, D., Nienow, P. W., Berthier, E., Vincent, C., Wagnon, P. and Trouvé, E.: Twenty-first century glacier slowdown driven by mass loss in High Mountain Asia, Nat. Geosci., 12, 22–27, doi:10.1038/s41561-018-0271-

9, 2019.

Dlugokencky, E., Lang, P., Mund, J., Crotwell, M. and Thoning, K.: Atmospheric Carbon Dioxide Dry Air Mole Fractions from the NOAA ESRL Carbon Cycle Cooperative Global Air Sampling Network, 1968-2017, , ftp://aftp.cmdl.noaa.gov/data/trace_gases/co2/flas, 2018.

Dong, W., Lin, Y., Wright, J. S., Xie, Y., Ming, Y., Zhang, H., Chen, R., Chen, Y., Xu, F., Lin, N., Yu, C., Zhang, B., Jin, S., Yang, K., Li, Z., Guo, J., Wang, L. and Lin, G.: Regional disparities in warm season rainfall changes over arid eastern – central Asia, Sci. Rep., 8(August), 13051, doi:10.1038/s41598-018-31246-3, 2018.

Dyer, A. J. and Hicks, B. B.: Flux-gradient relationships in the constant flux layer, Q. J. R. Meteorol. Soc., 96(410), 715–721, doi:10.1002/qj.49709641012, 1970.

Van der Esch, S., Ten Brink, B., Stehfest, E., Bakkenes, M., Sewell, A., Bouwman, A., Meijer, J., Westhoek, H. and Van den Berg, M.: Exploring future changes in land use and land condition and the impacts on food, water, climate change and biodiversity Scenarios for the UNCCD Global Land Outlook Policy Report, PBL Rep. http//www.pbl.nl/sites/default/files/cms/publicaties/pbl-2017-exploring-future-changes-in-land-use-and-land-condition-2076.pdf [online] Available from: http://www.pbl.nl/sites/default/files/cms/publicaties/pbl-2017-exploring-future-changes-in-land-use-and-land-condition-2076.pdf, 2017.

Fang, G., Chen, Y. and Li, Z.: Variation in agricultural water demand and its attributions in the arid Tarim River Basin, J. Agric. Sci., 156(3), 301–311, doi:10.1017/S0021859618000357, 2018.

Farinotti, D., Immerzeel, W. W., Kok, R. J. De, Quincey, D. J. and Dehecq, A.: Manifestations and mechanisms of the Karakoram glacier Anomaly, Nat. Geosci., 13(January), doi:10.1038/s41561-019-0513-5, 2020.

Forsythe, N., Fowler, H. J., Li, X.-F., Blenkinsop, S. and Pritchard, D.: Karakoram temperature and glacial melt driven by regional atmospheric circulation variability, Nat. Clim. Chang., (August), doi:10.1038/nclimate3361, 2017.

Fowler, H. J. and Archer, D. R.: Conflicting signals of climatic change in the upper Indus Basin, J. Clim., 19(17), 4276–4293, doi:10.1175/JCLI3860.1, 2006.

Gardelle, J., Berthier, E. and Arnaud, Y.: Slight mass gain of Karakoram glaciers in the early twenty-first century, Nat. Geosci., 5(5), 322–325, doi:10.1038/ngeo1450, 2012.

Gardelle, J., Berthier, E., Arnaud, Y. and Kääb, A.: Region-wide glacier mass balances over the Pamir-Karakoram-Himalaya during 1999-2011, Cryosphere, 7(4), 1263–1286, doi:10.5194/tc-7-1263-2013, 2013.

Hewitt, K.: The Karakoram Anomaly? Glacier Expansion and the 'Elevation Effect,' Karakoram Himalaya, Mt. Res. Dev., 25(4), 332–340, doi:10.1659/0276-4741(2005)025[0332:TKAGEA]2.0.CO;2, 2005.

Hong, S.-Y., Noh, Y. and Dudhia, J.: A new vertical diffusion package with an explicit treatment of entrainment processes., Mon. Weather Rev., 134(9), 2318–2341, doi:10.1175/MWR3199.1, 2006.

Iacono, M. J., Delamere, J. S., Mlawer, E. J., Shephard, M. W., Clough, S. A. and Collins, W. D.: Radiative forcing by long-lived greenhouse gases: Calculations with the AER radiative transfer models, J. Geophys. Res. Atmos., 113(13), 2–9, doi:10.1029/2008JD009944, 2008.

Immerzeel, W. W., Wanders, N., Lutz, A. F., Shea, J. M. and Bierkens, M. F. P.: Reconciling high-altitude precipitation in the upper Indus basin with glacier mass balances and runoff, Hydrol. Earth Syst. Sci., 19(11), 4673–4687, doi:10.5194/hess-19-4673-2015, 2015.

Jian, D., Li, X., Sun, H., Tao, H., Jiang, T., Su, B. and Hartmann, H.: Estimation of Actual Evapotranspiration by the Complementary Theory-Based Advection–Aridity Model in the Tarim River Basin, China, J. Hydrometeorol., 19(2), 289–303, doi:10.1175/JHM-D-16-0189.1, 2018.

Kääb, A., Treichler, D., Nuth, C. and Berthier, E.: Brief Communication: Contending estimates of 2003-2008 glacier mass balance over the Pamir-Karakoram-Himalaya, Cryosphere, 9(2), 557–564, doi:10.5194/tc-9-557-2015, 2015.

Kain, J. S.: The Kain–Fritsch Convective Parameterization: An Update, J. Appl. Meteorol., 43(1), 170–181, doi:10.1175/1520-0450(2004)043<0170:TKCPAU>2.0.CO;2, 2004.

Kapnick, S. B. S., Delworth, T. L. T., Ashfaq, M., Malyshev, S. and Milly, P. C. D.: Snowfall less sensitive to warming in Karakoram than in Himalayas due to a unique seasonal cycle, Nat. Geosci., 7(11), 834–840, doi:10.1038/ngeo2269, 2014.

Khattak, M. S., Babel, M. S. and Sharif, M.: Hydro-meteorological trends in the upper Indus River basin in Pakistan, Clim. Res., 46(2), 103–119, doi:10.3354/cr00957, 2011.

de Kok, R. J., Tuinenburg, O. A., Bonekamp, P. N. J. and Immerzeel, W. W.: Irrigation as a Potential Driver for Anomalous Glacier Behavior in High Mountain Asia, Geophys. Res. Lett., 45(4), 2047–2054, doi:10.1002/2017GL076158, 2018.

Kraaijenbrink, P. D. A., Bierkens, M. F. P., Lutz, A. F. and Immerzeel, W. W.: Impact of a global temperature rise of 1.5 degrees Celsius on Asia's glaciers, Nature, 549(7671), 257–260, doi:10.1038/nature23878, 2017.

Lawrimore, J. H., Menne, M. J., Gleason, B. E., Williams, C. N., Wuertz, D. B., Vose, R. S. and Rennie, J.: Global Historical Climatology Network - Monthly (GHCN-M), Version 3, , doi:10.7289/V5X34VDR, 2011.

Lee, E., Sacks, W. J., Chase, T. N. and Foley, J. A.: Simulated impacts of irrigation on the atmospheric circulation over Asia, J. Geophys. Res. Atmos., 116(8), 1–13, doi:10.1029/2010JD014740, 2011.

Lin, H., Li, G., Cuo, L., Hooper, A. and Ye, Q.: A decreasing glacier mass balance gradient from the edge of the Upper Tarim Basin to the Karakoram during 2000 – 2014, Sci. Rep., (December 2016), 1–9, doi:10.1038/s41598-017-07133-8, 2017.

Lobell, D. B., Bonfils, C. and Faurès, J. M.: The role of irrigation expansion in past and future temperature trends, Earth Interact., 12(3), 1–11, doi:10.1175/2007EI241.1, 2008.

Marshall, S. J., White, E. C., Demuth, M. N., Bolch, T., Wheate, R., Menounos, B., Beedle, M. J. and Shea, J. M.: Glacier water resources on the eastern slopes of the Canadian Rocky Mountains, Can. Water Resour. J., 36(2), 109–134, doi:10.4296/cwrj3602823, 2011.

Martens, B., Miralles, D. G., Lievens, H., Van Der Schalie, R., De Jeu, R. A. M., Fernández-Prieto, D., Beck, H. E., Dorigo, W. A. and Verhoest, N. E. C.: GLEAM v3: Satellite-based land evaporation and root-zone soil moisture, Geosci. Model Dev., 10(5), 1903–1925, doi:10.5194/gmd-10-1903-2017, 2017.

Maurer, J. M., Schaefer, J. M., Rupper, S. and Corley, A.: Acceleration of ice loss across the Himalayas over the past 40 years, Sci. Adv., 5, 1–12, doi:10.1126/sciadv.aav7266, 2019.

Maussion, F., Scherer, D., Mölg, T., Collier, E., Curio, J. and Finkelnburg, R.: Precipitation seasonality and variability over the Tibetan Plateau as resolved by the high Asia reanalysis, J. Clim., 27(5), 1910–1927, doi:10.1175/JCLI-D-13-00282.1, 2014.

Ménégoz, M., Gallée, H. and Jacobi, H. W.: Precipitation and snow cover in the Himalaya : from reanalysis to regional climate simulations, Hydrol. Earth Syst. Sci., 17, 3921–3936, doi:10.5194/hess-17-3921-2013, 2013.

Miralles, D. G., Gash, J. H., Holmes, T. R. H., De Jeu, R. A. M. and Dolman, A. J.: Global canopy interception from satellite observations, J. Geophys. Res. Atmos., 115(16), 1–8, doi:10.1029/2009JD013530, 2010.

Mölg, T., Maussion, F., Collier, E., Chiang, J. C. H. and Scherer, D.: Prominent midlatitude circulation signature in high Asia's surface climate during monsoon, J. Geophys. Res. Atmos., 122(23), 12,702-12,712, doi:10.1002/2017JD027414, 2017.

Morrison, H., Thompson, G. and Tatarskii, V.: Impact of Cloud Microphysics on the Development of Trailing Stratiform Precipitation in a Simulated Squall Line: Comparison of One- and Two-Moment Schemes, Mon. Weather Rev., 137(3), 991–1007, doi:10.1175/2008MWR2556.1, 2009.

Niu, G. Y., Yang, Z. L., Mitchell, K. E., Chen, F., Ek, M. B., Barlage, M., Kumar, A., Manning, K., Niyogi, D., Rosero, E., Tewari, M. and Xia, Y.: The community Noah land surface model with multiparameterization options (Noah-MP): 1. Model description and evaluation with local-scale measurements, J. Geophys. Res. Atmos., 116(12), 1–19, doi:10.1029/2010JD015139, 2011.

Norris, J., Carvalho, L. M. V., Jones, C. and Cannon, F.: WRF simulations of two extreme snowfall events associated with contrasting extratropical cyclones over the western and central Himalaya, J. Geophys. Res. Atmos., 120(8), 3114–3138, doi:10.1002/2014JD022592, 2015.

Norris, J., Carvalho, L. M. V., Jones, C. and Cannon, F.: Deciphering the contrasting climatic trends between the central Himalaya and Karakoram with 36 years of WRF simulations, Clim. Dyn., 52(0), 159, doi:10.1007/s00382-018-4133-3, 2018.

östrem, G.: Ice Melting under a Thin Layer of Moraine, and the Existence of Ice Cores in Moraine Ridges, Geogr. Ann., 41(4), 228–230, doi:10.1080/20014422.1959.11907953, 1959.

Otte, T. L., Nolte, C. G., Otte, M. J. and Bowden, J. H.: Does nudging squelch the extremes in regional climate modeling?, J. Clim., 25(20), 7046–7066, doi:10.1175/JCLI-D-12-00048.1, 2012.

Palazzi, E., Von Hardenberg, J. and Provenzale, A.: Precipitation in the hindu-kush karakoram himalaya: Observations and future scenarios, J. Geophys. Res. Atmos., 118(1), 85–100, doi:10.1029/2012JD018697, 2013.

Paulson, C. a.: The Mathematical Representation of Wind Speed and Temperature Profiles in the Unstable Atmospheric Surface Layer, J. Appl. Meteorol., 9(6), 857–861, doi:10.1175/1520-0450(1970)009<0857:TMROWS>2.0.CO;2, 1970.

Peng, D. and Zhou, T.: Why was the arid and semiarid Northwest China getting wetter in the recent decades?, J. Geophys. Res. Atmos., doi:10.1002/2016JD026424, 2017.

Peng, D., Zhou, T., Zhang, L. and Wu, B.: Human Contribution to the Increasing Summer Precipitation in Central Asia from 1961 to 2013, Clim. Dyn., 31, 8005–8021, doi:10.1175/JCLI-D-17-0843.1, 2018.

Pfeffer, W. T., Arendt, A. A., Bliss, A., Bolch, T., Cogley, J. G., Gardner, A. S., Hagen, J. O., Hock, R., Kaser, G., Kienholz, C., Miles, E. S., Moholdt, G., M??lg, N., Paul, F., Radi??, V., Rastner, P., Raup, B. H., Rich, J., Sharp, M. J., Andreassen, L. M., Bajracharya, S., Barrand, N. E., Beedle, M. J., Berthier, E., Bhambri, R., Brown, I., Burgess, D. O., Burgess, E. W., Cawkwell, F., Chinn, T., Copland, L., Cullen, N. J., Davies, B., De Angelis, H., Fountain, A. G., Frey, H., Giffen, B. A., Glasser, N. F., Gurney, S. D., Hagg, W., Hall, D. K., Haritashya, U. K., Hartmann, G., Herreid, S., Howat, I., Jiskoot, H., Khromova, T. E., Klein, A., Kohler, J., K??nig, M., Kriegel, D., Kutuzov, S., Lavrentiev, I., Le Bris, R., Li, X., Manley, W. F., Mayer, C., Menounos, B., Mercer, A., Mool, P., Negrete, A., Nosenko, G., Nuth, C., Osmonov, A., Pettersson, R., Racoviteanu, A., Ranzi, R., Sarikaya, M. A., Schneider, C., Sigurdsson, O., Sirguey, P., Stokes, C. R., Wheate, R., Wolken, G. J., Wu, L. Z. and Wyatt, F. R.: The randolph glacier inventory: A globally complete inventory of glaciers, J. Glaciol., 60(221), 537–552, doi:10.3189/2014JoG13J176, 2014.

Prinn, R. G., Weiss, R. F., Simmonds, P. J. F. P. G., Cunnold, D. M., Alyea, F. N., Doherty, S. O., Salameh, P., Miller, B. R., Huang, J., Wang, R. H. J., Hartley, D. E., Harth, C., Steele, L. P., Sturrock, G., Midgley, P. M. and Mcculloch, A.: A history of chemically and radiatively important gases in air deduced from ALE_GAGE_AGAGE, J. Geophys. Res. Atmos., 105(D14), 17,751-17,792, 2000.

Puma, M. J. and Cook, B. I.: Effects of irrigation on global climate during the 20th century, J. Geophys. Res. Atmos., 115(16), 1–15, doi:10.1029/2010JD014122, 2010.

Rodell, M., Houser, P. R., Jambor, U., Gottschalck, J., Mitchell, K., Meng, C.-J., Arsenault, K., Cosgrove, B., Radakovich, J., Bosilovich, M., Entin*, J. K., Walker, J. P., Lohmann, D. and Toll, D.: The Global Land Data Assimilation System, Bull. Am. Meteorol. Soc., 85(3), 381–394, doi:10.1175/BAMS-85-3-381, 2004.

Sacks, W. J., Cook, B. I., Buenning, N., Levis, S. and Helkowski, J. H.: Effects of global irrigation on the near-surface climate, Clim. Dyn., 33(2–3), 159–175, doi:10.1007/s00382-008-0445-z, 2009.

Sakai, A. and Fujita, K.: Contrasting glacier responses to recent climate change in high-mountain Asia, Sci. Rep., 7(1), 13717, doi:10.1038/s41598-017-14256-5, 2017.

Senay, G. B.: Satellite psychrometric formulation of the operational simplified surface energy balance (SSEBOP) model for quantiying and mapping evapotranspiration, Appl. Eng. Agric., 34(3), 555–566, doi:doi: 10.13031/aea.12614, 2018.

Siebert, S., Burke, J., Faures, J. M., Frenken, K., Hoogeveen, J., Döll, P. and Portmann, F. T.: Groundwater use for irrigation - A global inventory, Hydrol. Earth Syst. Sci., 14(10), 1863–1880, doi:10.5194/hess-14-1863-2010, 2010.

Skamarock, W. C. and Klemp, J. B.: A time-split nonhydrostatic atmospheric model for weather research and forecasting applications, J. Comput. Phys., 227(7), 3465–3485, doi:10.1016/j.jcp.2007.01.037, 2008.

Tuinenburg, O. A., Hutjes, R. W. A. and Kabat, P.: The fate of evaporated water from the Ganges basin, J. Geophys. Res. Atmos., 117(1), 1–17, doi:10.1029/2011JD016221, 2012.

Ul Hasson, S., Böhner, J. and Lucarini, V.: Prevailing climatic trends and runoff response from Hindukush-Karakoram-Himalaya, upper Indus Basin, Earth Syst. Dyn., 8(2), 337–355, doi:10.5194/esd-8-337-2017, 2017.

Wada, Y., Van Beek, L. P. H., Viviroli, D., Drr, H. H., Weingartner, R. and Bierkens, M. F. P.: Global monthly water stress: 2. Water demand and severity of water stress, Water Resour. Res., 47(7), 1–17, doi:10.1029/2010WR009792, 2011.

Wada, Y., Wisser, D. and Bierkens, M. F. P.: Global modeling of withdrawal, allocation and consumptive use of surface water and groundwater resources, Earth Syst. Dyn., 5(1), 15–40, doi:10.5194/esd-5-15-2014, 2014.

Wang, R., Liu, S., Shangguan, D., Radic, V. and Zhang, Y.: Spatial Heterogeneity in Glacier Mass-Balance Sensitivity across High Mountain Asia, Water, 11, 776, doi:10.3390/w11040776, 2019.

Waqas, A. and Athar, H.: Recent decadal variability of daily observed temperatures in Hindukush , Karakoram and Himalaya region in northern Pakistan, Clim. Dyn., 0(0), 0, doi:10.1007/s00382-018-4557-9, 2018.

Webb, E. K.: Profile relationships: The log-linear range, and extension to strong stability, Q. J. R. Meteorol. Soc., 96(407), 67–90, doi:10.1002/qj.49709640708, 1970.

Xu, Z., Liu, Z., Fu, G. and Chen, Y.: Trends of major hydroclimatic variables in the Tarim River basin during the past 50 years, J. Arid Environ., 74(2), 256–267, doi:10.1016/j.jaridenv.2009.08.014, 2010.

Zhang, D. and Anthes, R. A.: A High-Resolution Model of the Planetary Boundary Layer—Sensitivity Tests and Comparisons with SESAME-79 Data, J. Appl. Meteorol., 21(11), 1594–1609, doi:10.1175/1520-0450(1982)021<1594:AHRMOT>2.0.CO;2, 1982.